Materials and methods

This investigation conforms with the *Guide for the Care and Use of Laboratory Animals* published by the US National Institutes of Health (NIH Publication No. 85-23, revised 1996).

Surgical preparation

Twenty-four adult cats weighing from 2.2 to 3.8 kg were anesthetized by an intraperitoneal injection of pentobarbital sodium (30–35 mg/kg) and ventilated mechanically with room air mixed with oxygen. The depth of anesthesia was maintained with a continuous intravenous infusion of pentobarbital sodium (1–2 mg kg^{-1} h^{-1}) through a catheter inserted from the right femoral vein to the inferior vena cava. Systemic arterial pressure (AP) was monitored from a catheter inserted from the right femoral artery into the abdominal aorta. Heart rate (HR) was determined from an electrocardiogram using a cardiotachometer. Esophageal temperature of the animal was measured using a thermometer (CTM-303, TERUMO, Japan) and was maintained at around 37 °C using a heated pad and a lamp.

Bilateral vagal nerves were sectioned through a midline cervical incision. With the animal in the lateral position, the left fifth and sixth ribs were resected to expose the heart. A dialysis probe was implanted, using a fine guiding needle, into the anterolateral free wall of the left ventricle perfused by the left anterior descending coronary artery (LAD). A 3-0 silk suture was passed around the LAD just distal to the first diagonal branch for later coronary occlusion. When an experimental protocol required electrical stimulation of the vagal efferent nerves, bipolar platinum electrodes were attached to the cardiac end of sectioned vagal nerves bilaterally. The nerves and electrodes were covered with warmed mineral oil for insulation. When an experimental protocol required cardiac pacing, bipolar stainless-steel wire electrodes were sutured at the left ventricular apex away from the implanted dialysis probe. Heparin sodium (100 U/kg) was administered intravenously to prevent blood coagulation.

In additional four anesthetized cats, the left ventricle was implanted with a dialysis probe and a pair of pacing electrodes to examine the effects of left ventricular pacing alone on the myocardial interstitial NE levels. The dialysis probe and pacing leads were placed in the same manner as described in the previous paragraph.

At the end of the experiment, the experimental animals were killed with an overdose of pentobarbital sodium. Postmortem examination confirmed that the dialysis probe had been implanted within the left ventricular myocardium.

Dialysis technique

The materials and properties of the dialysis probe have been previously described (Akiyama et al., 1991, 1994). Briefly, we designed a transverse dialysis probe. A dialysis fiber (13 mm length, 310 μm O.D., 200 μm I.D.; PAN-1200, 50,000 molecular weight cutoff, Asahi Chemical, Japan) was glued at both ends to polyethylene tubes (25 cm length, 500 μm O.D., 200 μm I.D.). The dialysis probe was perfused at a rate of 2 μl/min with Ringer solution containing the cholinesterase inhibitor eserine (100 μM). Dialysate sampling was initiated 2 h after implanting the dialysis probe, when the dialysate concentrations of NE and ACh had reached steady states (Akiyama et al., 1991, 1994). The actual dialysate sampling lagged behind a given collection period by 5 min taking into account the dead space volume between the dialysis membrane and the sample tube. Dialysate concentrations of NE and ACh were measured separately by high performance liquid chromatography with electrochemical detection (DTA-300, Eicom, Japan). Details of the NE and ACh measurements have been previously described (Akiyama et al., 1991, 1994).

Protocols

Protocol 1 (VX, n = 8)

As a control experiment, we measured ischemia-induced NE and ACh releases during 60-min LAD occlusion in vagotomized animals. After collecting a 15-min baseline dialysate sample, we occluded the LAD for 60 min and collected four consecutive 15-min dialysate samples during acute myocardial ischemia. We then loosened the LAD snare and collected a 15-min dialysate sample during reperfusion.

Protocol 2 (VS, n = 8)

We examined the effects of vagal stimulation on ischemia-induced NE and ACh releases. To avoid possible preconditioning mimetic effects of ACh released by vagal stimulation (Przyklenk and Kloner, 1995; Kawada et al., 2002a), we initiated the bilateral vagal stimulation (5 Hz, 1 ms in pulse duration and 10 V in pulse amplitude) at the onset of LAD occlusion. The vagal stimulation continued for the 60-min ischemic period and the 15-min reperfusion period.

Protocol 3 (VSP, n = 8)

To eliminate the effects of bradycardia associated with vagal stimulation, we performed vagal stimulation under fixed-rate pacing conditions. We initiated the bilateral vagal stimulation (5 Hz, 1 ms in pulse duration and 10 V in pulse amplitude) and paced the heart from the onset of LAD occlusion to the conclusion of the experimental period. The ventricular pacing rate was set close to the HR recorded immediately before the LAD occlusion.

Supplemental protocol (n = 4)

To examine the effects of left ventricular pacing on the myocardial interstitial NE levels, we collected 15-min dialysate samples under control conditions as well as under left ventricular pacing at 170 beats/min.

Statistical analysis

All data are presented as means ± SE values. In each group, the effects of LAD occlusion on dialysate concentrations of NE and ACh were examined using a repeated-measures analysis of

variance followed by a Dunnett test against respective baseline concentrations. Because the variance of NE data was very large and increased with mean, the NE data were compared after the logarithmic transform (Snedecor and Cochran, 1989). Differences were considered significant at $P<0.05$. To examine the effects of vagal stimulation with or without the ventricular pacing, dialysate concentrations of NE and ACh were compared among the three groups at each corresponding time period using one-way analysis of variance followed by a Student–Newman–Keuls test for all pairwise comparisons (Glantz, 2002). The NE data were compared after the logarithmic transform. Differences were considered significant at $P<0.05$. Heart rate and mean AP were determined immediately before the coronary occlusion (designated as time 0), after 5, 10, 15, 30, 45, and 60 min of the occlusion, and after 15 min of reperfusion. One-way analysis of variance followed by a Student–Newman–Keuls test was also applied to compare HR and mean AP among the three groups at each time point.

Results

Fig. 1 depicts LAD occlusion-induced myocardial interstitial NE accumulation within the ischemic zone. The inset shows the NE levels during baseline conditions in a magnified ordinate. In the VX group, LAD occlusion increased the NE level approximately 200 fold compared to the baseline level at 45–60 min. This occlusion-induced NE accumulation was significantly suppressed in the VS group compared with the VX group in 15–30, 30–45, and 45–60 min time periods. The difference between the VS and VX groups did not reach statistical significance at the reperfusion period. In the VSP group, in which HR was kept constant, vagal stimulation did not attenuate the occlusion-induced NE accumulation. In the supplemental protocol, the baseline myocardial interstitial NE level was 0.17±0.01 nM. The NE level during ventricular pacing at 170 beats/min was 0.21±0.09 nM.

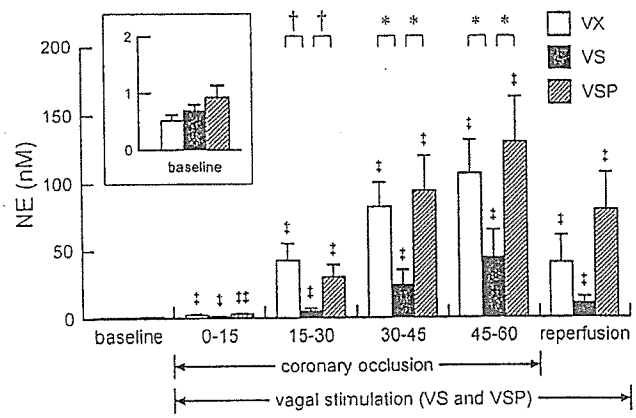

Fig. 1. Coronary occlusion-induced norepinephrine (NE) accumulation in the ischemic myocardium. VX: vagotomy, VS: vagal stimulation, VSP: vagal stimulation with ventricular pacing. The inset shows the baseline conditions with a magnified ordinate. Data are means±SE. ‡$P<0.01$ and ‡‡$P<0.05$ from the corresponding baseline value in each group. †$P<0.01$ and *$P<0.05$ by all pairwise comparisons among the three groups.

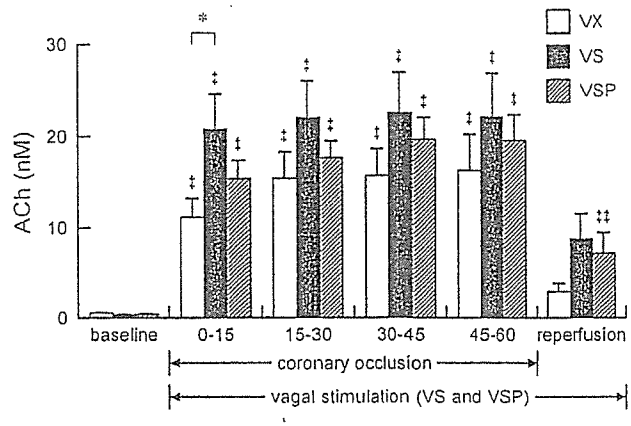

Fig. 2. Coronary occlusion-induced acetylcholine (ACh) accumulation in the ischemic myocardium. Data are means±SE. ‡$P<0.01$ and ‡‡$P<0.05$ from the corresponding baseline value in each group. *$P<0.05$ by all pairwise comparisons among the three groups.

Fig. 2 shows LAD occlusion-induced myocardial interstitial ACh accumulation within the ischemic zone. In the VX group, LAD occlusion increased the ACh level approximately 20 times higher than the baseline level at 45–60 min. The ACh level at 0–15 min was significantly higher in the VS than the VX group. For the rest of the ischemic period and reperfusion period, the differences between the VS and VX groups were not significant. The ACh levels in the VSP group did not differ from the VX group for any of the sampling periods.

Fig. 3 summarizes changes in HR and mean AP. In the VS group, HR was decreased by approximately 80 beats/min compared with the VX group at 5 min of coronary occlusion. The HR decrease continued for the rest of the ischemic period and reperfusion period. In the VSP group, HR was kept close to the preocclusion level, and it did not differ from the VX group

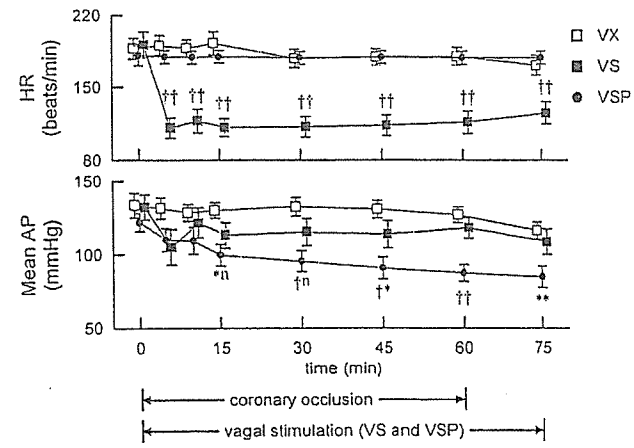

Fig. 3. Time courses of heart rate (HR) and mean arterial pressure (AP) during 60-min ischemia and 15-min reperfusion. The baseline values obtained just before coronary occlusion are plotted at time 0. Data points for VX and VSP groups are slightly displaced along the time axis for better view of overlapping points. Data are means±SE. In the HR data, †† represents statistical significance of $P<0.01$ from both the VX and VSP groups by all pairwise comparisons. In the AP data, when two characters are added to the VSP data point, the first and second characters represent the statistical significance from VX and VS groups, respectively. *, †, and n designate $P<0.05$, $P<0.01$, and "not significant", respectively.

for all the time points. Mean AP did not differ statistically between VX and VS groups. Mean AP in the VSP group progressively decreased and became significantly lower than the VX group after 15 min of the ischemic period. Mean AP in the VSP group was also significantly lower than the VS group after 45 min of the ischemic period.

Discussion

We have shown that electrical vagal stimulation suppressed ischemia-induced NE release and enhanced an initial increase in the ACh levels in the ischemic myocardium. Fixed-rate pacing abolished the suppression of ischemia-induced NE release by vagal stimulation in the present experimental settings.

Effects of vagal stimulation on ischemia-induced NE release

Several mechanisms can be put forward to explain the suppression of ischemia-induced myocardial interstitial NE release by vagal stimulation. First, activation of presynaptic muscarinic receptors on the sympathetic nerve endings inhibits the exocytotic NE release under normal physiological conditions (Levy and Blattberg, 1976). However, the presynaptic inhibition is unlikely the mechanism underlying the vagally mediated suppression of the ischemia-induced NE release because of the following reasons. Although the exocytotic release mechanism participates in the ischemia-induced NE release within the first 20 min of ischemia, the non-exocytotic release mechanism becomes predominant as the ischemic period is prolonged (Akiyama and Yamazaki, 1999). Myocardial ischemia gradually depletes ATP in the ischemic region including sympathetic nerve terminals, which leads to accumulation of axoplasmic NE and reduction of normal Na^+gradient across the plasma membrane in the sympathetic nerve terminals. The NE uptake transporter on the sympathetic nerve terminals, driven by the Na^+gradient, is then reversed, evoking non-exocytotic NE release (Schwartz, 2000). Therefore, the presynaptic inhibition of exocytotic NE release might contribute little to the suppression of ischemia-induced NE release during prolonged ischemia. Furthermore, the presynaptic inhibition of exocytotic NE release becomes less effective during the ischemic insult (Du et al., 1990; Haunstetter et al., 1994). The fact that the ischemia-induced NE release did not differ between the VSP and VX groups is also in opposition to the presynaptic inhibition as a chief mechanism underlying the vagally mediated suppression of ischemia-induced NE release (Fig. 1). Although left ventricular pacing could have affected myocardial interstitial NE levels, the results of the supplemental protocol indicates that changes in the NE levels by ventricular pacing might be negligibly small compared to the ischemia-induced NE release.

Second, the suppression of ischemia-induced NE release by vagal stimulation may be related to myocardial protection via direct vasodiation of the coronary artery. The coronary dilation may enhance collateral flow in the ischemic region and protect against myocardial deterioration evoked by ischemia. Both ACh and vasoactive intestinal polypeptide (VIP) are known to exert direct coronary dilation (Feliciano and Henning, 1998; Gross et al., 1981; Henning and Sawmiller, 2001). VIP is colocalized with ACh in the postganglionic vagal fibers and is released by high-frequency (20 Hz) vagal stimulation. VIP may interact with NE transport or exocytosis like nociceptin (Yamazaki et al., 2001). However, fixed-rate pacing abolished the ability of vagal stimulation to suppress the ischemia-induced NE release. Hence the direct coronary vasodilation and/or interaction with the sympathetic system via VIP might have played little role in suppressing ischemia-induced NE release in the present experimental settings. Another factor that should be taken into account is that the relatively low-frequency (5 Hz) stimulation might have limited the amount of VIP release from the vagal nerve endings.

Third, HR is one of the most important determinants of myocardial oxygen consumption (Mohrman and Heller, 1997). In the present study, HR in the VS group decreased to approximately 60% that of the VX group during the ischemic period (Fig. 3), which slowed the energy consumption of the myocardium. Bradycardia might also decrease ventricular contractility via a force-frequency mechanism (Maughan et al., 1985). In addition, bradycardia may increase coronary perfusion via prolongation of diastolic interval (Buck et al., 1981). These factors slowed energy consumption in the ischemic region including sympathetic nerve terminals, delaying the time course for non-exocytotic NE release. The prevention of excess NE would further reduce myocardial oxygen consumption and decelerate the progression of ischemic injury (Suga et al., 1983). The ischemia-induced NE release did not differ between the VSP and VX groups despite the lower mean AP in the VSP compared with the VX group. Although lowering AP might decrease afterload of the ventricle and reduce energy consumption, the beneficial effect of afterload reduction might have been masked in the VSP group due to inefficient cardiac pumping function associated with asynchrony between sinus rate and ventricular rate. Proper atrioventricular conduction time contributes to the ventricular filling (Meisner et al., 1985). In the VSP group, the sinus rate was reduced by vagal stimulation whereas the ventricular rate was maintained by fixed-rate pacing. Dissociation of the sinus rate and ventricular rate might have impaired the ventricular filling to a variable extent, resulting in a progressive reduction in AP.

Finally, the vagal stimulation decreases ventricular contractile force against sympathetic activation via the direct projections to the ventricle (Nakayama et al., 2001). This mechanism might have also contributed to the reduction of the myocardial oxygen consumption and slowed the progression of ischemic injury in the VS group. However, the ventricular pacing canceled the protective effects in the VSP group, possibly by the adverse influences discussed in the previous paragraph. Further studies are required to isolate the factor(s) most important for the suppression of ischemia-induced NE release by the vagal stimulation.

Effects of vagal stimulation on ischemia-induced ACh release

In contrast to the suppressive effect of NE release, vagal nerve stimulation can exert two opposing influences on ACh release in the ischemic myocardium. The nerve stimulation itself induces exocytotic ACh release from nerve endings. Acute myocardial ischemia impairs conduction of the nerves traversing in the ischemic region (Barber et al., 1983; Inoue and Zipes, 1988; Martins et al., 1989). Acute myocardial ischemia also impairs the exocytotic ACh release in the postischemic myocardium (Kawada et al., 2002b). On the other hand, acute myocardial ischemia causes myocardial ACh release in the ischemic region via a local release mechanism independent of efferent nerve activity (Kawada et al., 2000). Hence, the amount of ACh release was net effects of ACh release evoked by nerve stimulation and ischemia; vagally mediated protection against ischemic injury should augment the former and attenuate the latter.

Although vagal stimulation augmented myocardial interstitial ACh release during the 0–15 min period of coronary occlusion in the VS group than in the VX group, the initial enhancement was not observed in the VSP group. One possible mechanism for the difference in the initial ACh release between the VS and VSP groups is that the progression of ischemia in the VSP group relative to the VS group impaired the vagal nerve conduction in the ischemic region, reducing the exocytotic ACh release. The other possible mechanism is that the high levels of NE might have attenuated the stimulation-induced ACh release from the vagal nerve endings via α-adrenergic mechanisms (Akiyama and Yamazaki, 2000).

There are several limitations to the present study. First, we avoided large myocardial ischemia by occluding LAD just distal to the first diagonal branch. Accordingly, the incidence of lethal ventricular arrhythmia was too low to draw any conclusion as to the effects of vagal stimulation on the arrhythmogenesis. Further studies with larger myocardial ischemia are clearly required to examine the effects of vagal stimulation on the incidence of lethal ventricular arrhythmia in relation to the observed NE and/or ACh levels in the ischemic myocardium. Second, plasma catecolamine levels might have been increased during the LAD occlusion, which might affect HR and cardiac function in the non-ischemic region. Although changes in plasma catecholamine levels may play significant roles in determining systemic hemodynamics, the ischemic region was only poorly perfused. Accordingly, direct effects of plasma catecholamines on the myocardial interstitial NE and ACh levels in the ischemic region might have been limited in the present study.

Conclusion

Electrical vagal stimulation suppressed ischemia-induced NE release in the ischemic myocardium in anesthetized cats. The vagal stimulation augmented ischemia-induced ACh release at the 0–15 min period of ischemia. Although acute myocardial ischemia causes myocardial NE and ACh releases independent of efferent nerve activity, the vagal stimulation was able to modulate both NE and ACh levels in the ischemic region. The suppression of NE release and augmentation of initial ACh release in the ischemic myocardium by vagal stimulation may reduce the ischemic injury to the heart. The direct neural intervention could be a new modality of medical engineering to cope with ischemic heart diseases.

Acknowledgments

This study was supported by Health and Labour Sciences Research Grant for Research on Advanced Medical Technology (H14-Nano-002) from the Ministry of Health Labour and Welfare of Japan, by Grant-in-Aid for Scientific Research (C-15590786) from the Ministry of Education, Science, Sports and Culture of Japan, and by the Program for Promotion of Fundamental Studies in Health Science from the Organization for Pharmaceutical Safety and Research.

References

Akiyama, T., Yamazaki, T., 1999. Norepinephrine release from cardiac sympathetic nerve endings in the in vivo ischemic region. Journal of Cardiovascular Pharmacology 34, S11–S14.

Akiyama, T., Yamazaki, T., 2000. Adrenergic inhibition of endogenous acetylcholine release on postganglionic cardiac vagal nerve terminals. Cardiovascular Research 46, 531–538.

Akiyama, T., Yamazaki, T., Ninomiya, I., 1991. In vivo monitoring of myocardial interstitial norepinephrine by dialysis technique. American Journal of Physiology. Heart and Circulatory Physiology 261, H1643–H1647.

Akiyama, T., Yamazaki, T., Ninomiya, I., 1994. In vivo detection of endogenous acetylcholine release in cat ventricles. American Journal of Physiology. Heart and Circulatory Physiology 266, H854–H860.

Armour, J.A., 1999. Myocardial ischaemia and the cardiac nervous system. Cardiovascular Research 41, 41–54.

Barber, M.J., Mueller, T.M., Henry, D.P., Felten, S.Y., Zipes, D.P., 1983. Transmural myocardial infarction in the dog produces sympathectomy in noninfarcted myocardium. Circulation 67, 787–796.

Buck, J.D., Warltier, D.C., Hardman, H.F., Gross, G.J., 1981. Effects of sotalol and vagal stimulation on ischemic myocardial blood flow distribution in the canine heart. Journal of Pharmacological and Experimental Therapeutics 216, 347–351.

Du, X.J., Dart, A.M., Riemersma, R.A., Oliver, M.F., 1990. Failure of the cholinergic modulation of norepinephrine release during acute myocardial ischemia in the rat. Circulation Research 66, 950–956.

Feliciano, L., Henning, R.J., 1998. Vagal nerve stimulation releases vasoactive intestinal peptide which significantly increases coronary artery blood flow. Cardiovascular Research 40, 45–55.

Glantz, S.A., 2002. Primer of Biostatistics, 5th ed. McGraw-Hill, New York.

Gross, G.J., Buck, J.D., Warltier, D.C., 1981. Transmural distribution of blood flow during activation of coronary muscarinic receptors. American Journal of Physiology. Heart and Circulatory Physiology 240, H941–H946.

Haunstetter, A., Haass, M., Yi, X., Krüger, C., Kübler, W., 1994. Muscarinic inhibition of cardiac norepinephrine and neuropeptide Y release during ischemia and reperfusion. American Journal of Physiology. Regulatory, Integrative and Comparative Physiology 267, R1552–R1558.

Henning, R.J., Sawmiller, D.R., 2001. Vasoactive intestinal peptide: cardiovascular effects. Cardiovascular Research 49, 27–37.

Inoue, H., Zipes, D.P., 1988. Time course of denervation of efferent sympathetic and vagal nerves after occlusion of the coronary artery in the canine heart. Circulation Research 62, 1111–1120.

Kawada, T., Yamazaki, T., Akiyama, T., Sato, T., Shishido, T., Inagaki, M., Takaki, H., Sugimachi, M., Sunagawa, K., 2000. Differential acetylcholine release mechanisms in the ischemic and non-ischemic myocardium. Journal of Molecular and Cellular Cardiology 32, 405–414.

Kawada, T., Yamazaki, T., Akiyama, T., Inagaki, M., Shishido, T., Zheng, C., Yanagiya, Y., Sugimachi, M., Sunagawa, K., 2001. Vagosympathetic interactions in ischemia-induced myocardial norepinephrine and acetylcholine release. American Journal of Physiology. Heart and Circulatory Physiology 280, H216–H221.

Kawada, T., Yamazaki, T., Akiyama, T., Mori, H., Inagaki, M., Shishido, T., Takaki, H., Sugimachi, M., Sunagawa, K., 2002. Effects of brief ischaemia on myocardial acetylcholine and noradrenaline levels in anaesthetized cats. Autonomic Neuroscience 95, 37–42.

Kawada, T., Yamazaki, T., Akiyama, T., Mori, H., Uemura, K., Miyamoto, T., Sugimachi, M., Sunagawa, K., 2002. Disruption of vagal efferent axon and nerve terminal function in the postischemic myocardium. American Journal of Physiology. Heart and Circulatory Physiology 283, H2687–H2691.

Lameris, T.W., de Zeeuw, Sandra, Alberts, G., Boomsma, F., Duncker, D.J., Verdouw, P.D., Veld, A.J., van den Meiracker, A.H., 2000. Time course and mechanism of myocardial catecholamine release during transient ischemia in vivo. Circulation 101, 2645–2650.

Levy, M.N., Blattberg, B., 1976. Effect of vagal stimulation on the overflow of norepinephrine into the coronary sinus during cardiac sympathetic nerve stimulation in the dog. Circulation Research 38, 81–84.

Li, M., Zheng, C., Sato, T., Kawada, T., Sugimachi, M., Sunagawa, K., 2004. Vagal nerve stimulation markedly improves long-term survival after chronic heart failure in rats. Circulation 109, 120–124.

Martins, J.B., Lewis, R., Wendt, D., Lund, D.D., Schmid, P.G., 1989. Subendocardial infarction produces epicardial parasympathetic denervation in canine left ventricle. American Journal of Physiology. Heart and Circulatory Physiology 256, H859–H866.

Maughan, W.L., Sunagawa, K., Burkhoff, D., Graves, W.L. Jr., Hunter, W.C., Sagawa, K., 1985. Effect of heart rate on the canine end-systolic pressure–volume relationship. Circulation 72, 654–659.

Meisner, J.S., McQueen, D.M., Ishida, Y., Vetter, H.O., Bortolotti, U., Strom, J.A., Frater, R.W.M., Peskin, C.S., Yellin, E.L., 1985. Effects of timing of atrial systole on LV filling and mitral valve closure: computer and dog studies. American Journal of Physiology. Heart and Circulatory Physiology 249, H604–H619.

Mohrman, D.E., Heller, L.J., 1997. Cardiovascular Physiology, 4th ed. McGraw-Hill, New York, pp. 47–69.

Nakayama, Y., Miyano, H., Shishido, T., Inagaki, M., Kawada, T., Sugimachi, M., Sunagawa, K., 2001. Heart rate-independent vagal effect on end-systolic elastance of the canine left ventricule under various levels of sympathetic tone. Circulation 104, 2277–2279.

Przyklenk, K., Kloner, R.A., 1995. Low-dose i.v. acetylcholine acts as a "preconditioning-mimetic" in the canine model. Journal of Cardiac Surgery 10, 389–395.

Rosenshtraukh, L., Danilo Jr., P., Anyukhovsky, E.P., Steinberg, S.F., Rybin, V., Brittain-Valenti, K., Molina-Viamonte, V., Rosen, M.R., 1994. Mechanisms for vagal modulation of ventricular repolarization and of coronary occlusion-induced lethal arrhythmias in cats. Circulation Research 75, 722–732.

Schömig, A., Fischer, S., Kurz, T., Richardt, G., Schömig, E., 1987. Nonexocytotic release of endogenous noradrenaline in the ischemic and anoxic rat heart: mechanism and metabolic requirements. Circulation Research 60, 194–205.

Schwartz, J.H., 2000. Neurotransmitters. In: Kandel, E.R., Schwartz, J.H., Jessell, T.M. (Eds.), Principles of Neural Science, 4th ed. McGraw-Hill, New York, pp. 280–297.

Snedecor, G.W., Cochran, W.G., 1989. Statistical Methods, 8th ed. Iowa State, Iowa, pp. 290–291.

Suga, H., Hisano, R., Goto, Y., Yamada, O., Igarashi, Y., 1983. Effect of positive inotropic agents on the relation between oxygen consumption and systolic pressure volume area in canine left ventricle. Circulation Research 53, 306–318.

Vanoli, E., De Ferrari, G.M., Stramba-Badiale, M., Hull Jr., S.S., Foreman, R.D., Schwartz, P.J., 1991. Vagal stimulation and prevention of sudden death in conscious dogs with a healed myocardial infarction. Circulation Research 68, 1471–1481.

Yamazaki, T., Akiyama, T., Kitagawa, H., Takauchi, Y., Kawada, T., Sunagawa, K., 1997. A new, concise dialysis approach to assessment of cardiac sympathetic nerve terminal abnormalities. American Journal of Physiology. Heart and Circulatory Physiology 272, H1182–H1187.

Yamazaki, T., Akiyama, T., Mori, H., 2001. Effects of nociceptin on cardiac norepinephrine and acetylcholine release evoked by ouabain. Brain Research 904, 153–156.

Am J Physiol Heart Circ Physiol 291: H2187–H2191, 2006.
First published June 9, 2006; doi:10.1152/ajpheart.00175.2006.

Effects of Ca^{2+} channel antagonists on nerve stimulation-induced and ischemia-induced myocardial interstitial acetylcholine release in cats

Toru Kawada,[1] Toji Yamazaki,[2] Tsuyoshi Akiyama,[2] Kazunori Uemura,[1] Atsunori Kamiya,[1] Toshiaki Shishido,[1] Hidezo Mori,[2] and Masaru Sugimachi[1]

[1]Department of Cardiovascular Dynamics, Advanced Medical Engineering Center, National Cardiovascular Center Research Institute and [2]Department of Cardiac Physiology, National Cardiovascular Center Research Institute, Osaka, Japan

Submitted 17 February 2006; accepted in final form 7 June 2006

Kawada, Toru, Toji Yamazaki, Tsuyoshi Akiyama, Kazunori Uemura, Atsunori Kamiya, Toshiaki Shishido, Hidezo Mori, and Masaru Sugimachi. Effects of Ca^{2+} channel antagonists on nerve stimulation-induced and ischemia-induced myocardial interstitial acetylcholine release in cats. *Am J Physiol Heart Circ Physiol* 291: H2187–H2191, 2006. First published June 9, 2006; doi:10.1152/ajpheart.00175.2006.—Although an axoplasmic Ca^{2+} increase is associated with an exocytotic acetylcholine (ACh) release from the parasympathetic postganglionic nerve endings, the role of voltage-dependent Ca^{2+} channels in ACh release in the mammalian cardiac parasympathetic nerve is not clearly understood. Using a cardiac microdialysis technique, we examined the effects of Ca^{2+} channel antagonists on vagal nerve stimulation- and ischemia-induced myocardial interstitial ACh releases in anesthetized cats. The vagal stimulation-induced ACh release [22.4 nM (SD 10.6), $n = 7$] was significantly attenuated by local administration of an N-type Ca^{2+} channel antagonist ω-conotoxin GVIA [11.7 nM (SD 5.8), $n = 7$, $P = 0.0054$], or a P/Q-type Ca^{2+} channel antagonist ω-conotoxin MVIIC [3.8 nM (SD 2.3), $n = 6$, $P = 0.0002$] but not by local administration of an L-type Ca^{2+} channel antagonist verapamil [23.5 nM (SD 6.0), $n = 5$, $P = 0.758$]. The ischemia-induced myocardial interstitial ACh release [15.0 nM (SD 8.3), $n = 8$] was not attenuated by local administration of the L-, N-, or P/Q-type Ca^{2+} channel antagonists, by inhibition of Na^+/Ca^{2+} exchange, or by blockade of inositol 1,4,5-trisphosphate [Ins(1,4,5)P_3] receptor but was significantly suppressed by local administration of gadolinium [2.8 nM (SD 2.6), $n = 6$, $P = 0.0283$]. In conclusion, stimulation-induced ACh release from the cardiac postganglionic nerves depends on the N- and P/Q-type Ca^{2+} channels (with a dominance of P/Q-type) but probably not on the L-type Ca^{2+} channels in cats. In contrast, ischemia-induced ACh release depends on nonselective cation channels or cation-selective stretch activated channels but not on L-, N-, or P/Q type Ca^{2+} channels, Na^+/Ca^{2+} exchange, or Ins(1,4,5)P_3 receptor-mediated pathway.

cardiac microdialysis; ω-conotoxin GVIA; ω-conotoxin MVIIC; KB-R7943; verapamil; vagal stimulation

ALTHOUGH N-TYPE Ca^{2+} CHANNELS play a dominant role in norepinephrine release from sympathetic nerve endings (8, 33, 34), the type(s) of Ca^{2+} channels controlling ACh release in the mammalian parasympathetic system is not fully understood and show diversity among reports. To name a few, in isolated parasympathetic submandibular ganglia from the rat, neurotransmission is mediated by Ca^{2+} channels that are resistant to the L-, N-, P/Q-, and R- type Ca^{2+} channel antagonists (29). When the negative inotropic response to field stimulation was examined in the isolated guinea pig atria, Hong and Chang (8) reported the importance of P/Q-type Ca^{2+} channels, whereas Serone et al. (28) reported the importance of N-type Ca^{2+} channels. Because field stimulation in the isolated preparations could induce responses different from those in the in vivo conditions, we aimed to examine the effects of Ca^{2+} channel antagonists on the vagal nerve stimulation-induced myocardial interstitial ACh release in the in vivo feline heart.

Aside from the important role of the normal physiological regulation of the heart, the vagal nerve can be a therapeutic target for certain cardiovascular diseases (2, 3, 13, 22, 27). In previous studies, we have shown that acute myocardial ischemia causes myocardial interstitial ACh release in the ischemic region independently of efferent vagal nerve activity (12, 14). The comparison of the effects of Ca^{2+} channel antagonists on the ACh releases induced by vagal nerve stimulation and by acute myocardial ischemia may deepen our understanding about the ischemia-induced myocardial interstitial ACh release.

A cardiac microdialysis technique offers detailed analyses of in vivo myocardial interstitial ACh release (1, 15). Because the local administration of pharmacological agents through a dialysis probe can modulate ACh release without significantly affecting systemic hemodynamics, a combination of cardiac microdialysis with local pharmacological interventions is useful for analyzing the mechanisms of ACh release in vivo. In the present study, we examined the effects of Ca^{2+} channel antagonists on nerve stimulation- and ischemia-induced ACh releases in anesthetized cats. The results indicate that stimulation-induced ACh release from the cardiac parasympathetic postganglionic nerves depends on the N- and P/Q-type Ca^{2+} channels but probably not on the L-type Ca^{2+} channels. In contrast, ischemia-induced myocardial interstitial ACh release is resistant to the inhibition of L-, N-, and P/Q-type Ca^{2+} channels. In addition, the ischemia-induced myocardial ACh release is resistant to the inhibition of Na^+/Ca^{2+} exchanger and the blockade of inositol 1,4,5-trisphosphate [Ins(1,4,5)P_3] receptor but is suppressed by gadolinium, suggesting that nonselective cation channels or cation-selective stretch-activated channels are involved.

MATERIALS AND METHODS

Common Preparation

Animal care was provided in accordance with the *Guiding Principles for the Care and Use of Animals in the Field of Physiological*

Address for reprint requests and other correspondence: T. Kawada, Dept. of Cardiovascular Dynamics, Advanced Medical Engineering Center, National Cardiovascular Center Research Institute, 5-7-1 Fujishirodai, Suita, Osaka 565-8565, Japan (e-mail: torukawa@res.ncvc.go.jp).

The costs of publication of this article were defrayed in part by the payment of page charges. The article must therefore be hereby marked "*advertisement*" in accordance with 18 U.S.C. Section 1734 solely to indicate this fact.

0363-6135/06 $8.00 Copyright © 2006 the American Physiological Society

Sciences approved by the Physiological Society of Japan. All protocols were approved by the Animal Subjects Committee of the National Cardiovascular Center. Adult cats weighing from 2.2 to 4.2 kg were anesthetized via an intraperitoneal injection of pentobarbital sodium (30–35 mg/kg) and ventilated mechanically with room air mixed with oxygen. The depth of anesthesia was maintained with a continuous intravenous infusion of pentobarbital sodium (1–2 mg·kg $^{-1}$·h $^{-1}$) through a catheter inserted from the right femoral vein. Systemic arterial pressure was monitored from a catheter inserted from the right femoral artery. The vagi were sectioned bilaterally at the neck. The esophageal temperature of the animal, which was measured by a thermometer (CTM-303, TERUMO, Japan), was maintained at around 37°C using a heated pad and a lamp.

With the animal in the lateral position, the left fifth and sixth ribs were resected to expose the heart. A dialysis probe was implanted transversely, using a fine guiding needle, into the anterolateral free wall of the left ventricle perfused by the left anterior descending coronary artery (LAD). Heparin sodium (100 U/kg) was administered intravenously to prevent blood coagulation. At the end of the experiment, the experimental animals were killed with an overdose of pentobarbital sodium. Postmortem examination confirmed that the dialysis probe had been threaded in the middle layer of the left ventricular myocardium. The thickness of the left ventricular free wall was ~7–8 mm, and the semipermeable membrane of the dialysis probe was positioned ~3–4 mm from the epicardial surface.

Dialysis Technique

The materials and properties of the dialysis probe have been described previously (1). Briefly, we designed a transverse dialysis probe. A dialysis fiber of semipermeable membrane (13 mm length, 310 μm OD, 200 μm ID; PAN-1200, 50,000 molecular weight cutoff, Asahi Chemical, Japan) was glued at both ends to polyethylene tubes (25 cm length, 500 μm OD, 200 μm ID). The dialysis probe was perfused at a rate of 2 μl/min with Ringer solution containing a cholinesterase inhibitor eserine (physostigmine, 100 μM). Experimental protocols were started 2 h after the dialysis probe was implanted when the ACh concentration in the dialysate reached a steady state. The ACh concentration in the dialysate was measured by high-performance liquid chromatography with electrochemical detection (Eicom, Kyoto, Japan).

Local administration of a pharmacological agent was carried out through a dialysis probe. That is to say, we added the pharmacological agent to the perfusate and allowed 1 h for a settling time. The pharmacological agent should spread around the semipermeable membrane, thereby affecting the neurotransmitter release in the vicinity of the semipermeable membrane. Because the distribution across the semipermeable membrane is required, based on previous results (33, 34), we used the pharmacological agent at the concentration 10–100 times higher than that required for complete channel blockade in experimental settings in vitro.

Specific Preparation and Protocols

Protocol 1. Bipolar platinum electrodes were attached bilaterally to the cardiac ends of the sectioned vagi at the neck. The nerves and electrodes were covered with warmed mineral oil for insulation. The vagal nerves were stimulated for 15 min (20 Hz, 1 ms, 10 V). We measured the stimulation-induced ACh release in the absence of Ca^{2+} channel blockade (control, n = 7) and examined the effects of an L-type Ca^{2+} channel antagonist verapamil (100 μM, n = 5), an N-type Ca^{2+} channel antagonist ω-conotoxin GVIA (10 μM, n = 7), a P/Q-type Ca^{2+} channel antagonist ω-conotoxin MVIIC (10 μM, n = 6), and combined administration of ω-conotoxin GVIA and ω-conotoxin MVIIC (10 μM each, n = 6).

Protocol 2. Because a preliminary result from *protocol 1* suggested that local administration of verapamil was ineffective in suppressing stimulation-induced ACh release, we examined the effects of the intravenous administration of verapamil (300 μg/kg, n = 6) on stimulation-induced ACh release in vagotomized animals as a supplemental experiment.

Protocol 3. A 60-min LAD occlusion was performed by using a 3-0 silk suture passed around the LAD just distal to the first diagonal branch. We measured the ACh levels during 45–60 min of ischemia in the absence of Ca^{2+} channel blockade (control, n = 8) and examined the effects of verapamil (100 μM, n = 5), ω-conotoxin GVIA (10 μM, n = 5), and ω-conotoxin MVIIC (10 μM, n = 5). A previous result indicated that the ischemia-induced ACh release reached the steady state during 45–60 min of ischemia (14). We also examined the effects of three additional agents, a Na^+/Ca^{2+} exchange inhibitor KB-R7943 (10 μM, n = 5) (9, 10), an Ins(1,4,5)P_3 receptor blocker xestospongin C (500 μM, n = 6) (25), and a nonselective cation channel blocker or a cation-selective stretch activated channel blocker gadolinium (1 mM) (5, 17), on the ischemia-induced ACh release.

Statistical Analysis

All data are presented as mean (SD) values. In *protocol 1*, we compared stimulation-induced ACh release among the five groups using one-way analysis of variance followed by the Student-Neuman-Keuls test (6). In *protocol 2*, we used an unpaired-t test (two-sided) to examine the effect of intravenous verapamil administration on stimulation-induced ACh release. In *protocol 3*, we compared ischemia-induced ACh release among the seven groups using one-way analysis of variance followed by the Dunnett' test against the control. For all analyses, differences were considered significant when $P < 0.05$.

RESULTS

In *protocol 1*, the ACh level during electrical vagal stimulation was 22.4 nM (SD 10.6). Local administration of verapamil did not affect stimulation-induced ACh release (Fig. 1). In contrast, local administration of ω-conotoxin GVIA or ω-conotoxin MVIIC suppressed stimulation-induced ACh release. The extent of suppression was greater in the latter. The ACh level was significantly lower in the simultaneous administration group (ω-conotoxin GVIA + ω-conotoxin MVIIC)

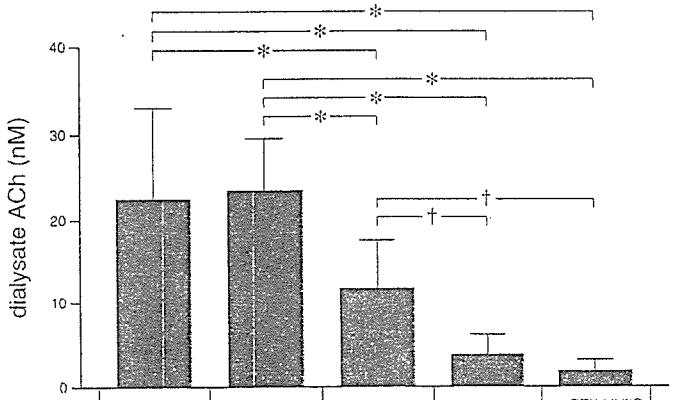

	vehicle	verapamil	ω-CTX GVIA	ω-CTX MVIIC	ω-CTX MVIIC + ω-CTX GVIA
vehicle		0.758	0.0054	0.0002	0.0002
verapamil	0.758		0.0068	0.0002	0.0001
GVIA	0.0054	0.0068		0.033	0.025
MVIIC	0.0002	0.0002	0.033		0.581
MVIIC+GVIA	0.0002	0.0001	0.025	0.581	

Fig. 1. Effects of local administration of verapamil, ω-conotoxin GVIA, ω-conotoxin MVIIC, or ω-conotoxin GVIA plus ω-conotoxin MVIIC on vagal nerve stimulation-induced myocardial interstitial ACh release. Both ω-conotoxin GVIA and ω-conotoxin MVIIC, but not verapamil, suppressed stimulation-induced ACh release. Data are mean (SD) values. *$P < 0.01$, †$P < 0.05$. The exact P values are presented.

than that in the ω-conotoxin GVIA group but was not different from the ω-conotoxin MVIIC group.

In *protocol 2*, the intravenous administration of verapamil did not significantly change stimulation-induced ACh release [21.7 nM (SD 12.8)] compared with the control group (P = 0.91).

In *protocol 3*, the ACh level in the ischemic region was 14.9 nM (SD 8.3) during 45–60 min of acute myocardial ischemia. Inhibition of voltage-dependent Ca^{2+} channels by local administration of verapamil, ω-conotoxin GVIA, or ω-conotoxin MVIIC did not affect ischemia-induced ACh release (Fig. 2). Inhibition of the reverse mode action of Na^{+}/Ca^{2+} exchange by local administration of KB-R7943 appeared to have augmented rather than suppressed ischemia-induced ACh release, though there was no statistically significant difference from the control. Blockade of the Ins(1,4,5)P_3 receptor by local administration of xestospongin C did not affect the ischemia-induced ACh release. In contrast, blockade of nonselective cation channels or cation-selective stretch-activated channels by local administration of gadolinium suppressed the ischemia-induced ACh release.

DISCUSSION

Ca^{2+} Channels Involved in Stimulation-Induced ACh Release

Although neurotransmitter release at mammalian sympathetic neuroeffector junctions predominantly depends on Ca^{2+} influx through N-type Ca^{2+} channels (23, 33, 34), the type(s) of Ca^{2+} channels involved in ACh release from cardiac parasympathetic neuroeffector junctions show diversity among reports (8, 28). One possible factor hampering investigations into parasympathetic postganglionic neurotransmitter release in response to vagal nerve stimulation in vivo is that the parasympathetic ganglia are usually situated in the vicinity of the effector organs, thereby making it difficult to separately assess ACh release from preganglionic and postganglionic nerves. In the previous study from our laboratory, intravenous administration, but not local administration of a ganglionic blocker, hexamethonium reduced vagal stimulation-induced ACh release assessed by cardiac microdialysis (1). The negligible effect of local hexamethonium administration on stimulation-induced ACh release suggests the lack of parasympathetic ganglia around the dialysis probe. In support of our speculation, a recent neuroanatomical finding indicates that three ganglia, away from the left anterior free wall targeted by the dialysis probe, provide the major source for left ventricular postganglionic innervation in cats: a cranioventricular ganglion, a left ventricular ganglion 2 (so designated), and an interventriculo-septal ganglion (11). Therefore, ACh, as measured by cardiac microdialysis, is considered to predominantly reflect ACh release from parasympathetic postganglionic nerves.

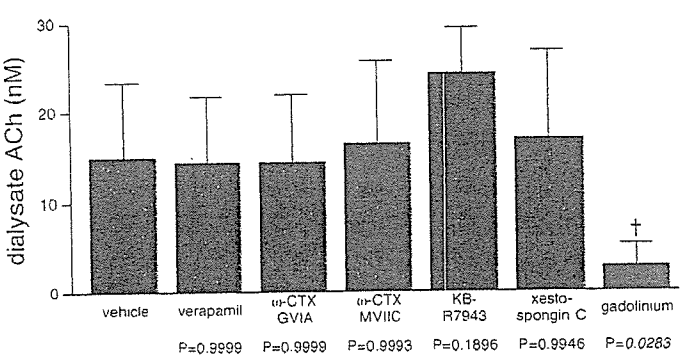

Fig. 2. Effects of local administration of verapamil, ω-conotoxin GVIA, ω-conotoxin MVIIC, KB-R7943, xestospongin C, or gadolinium on acute myocardial ischemia-induced myocardial interstitial ACh release in the ischemic region. Gadolinium alone suppressed the ischemia-induced ACh release. Data are mean (SD) values. †$P < 0.05$. The exact P values are presented.

Local (*protocol 1*) or intravenous (*protocol 2*) administration of verapamil did not affect stimulation-induced ACh release. In contrast, vagal stimulation-induced ACh release was reduced in both the ω-conotoxin GVIA and ω-conotoxin MVIIC groups but to a greater extent in the latter (Fig. 1). Therefore, both N- and P/Q-type, but probably not L-type, Ca^{2+} channels are involved in stimulation-induced ACh release from the cardiac parasympathetic postganglionic nerves in cats. The contribution of P/Q type Ca^{2+} channels to ACh release might be greater than that of N-type Ca^{2+} channels. Hong and Chang (8) reported that the negative inotropic response to field stimulation depends predominantly on the P/Q-type Ca^{2+} channels in isolated guinea pig atria, whereas Serone et al. (28) reported the predominance of N-type Ca^{2+} channels. In those studies, the field stimulation employed differed from ordinary activation of the postganglionic nerves by nerve discharge and, in addition, ACh release was not directly measured. The present study directly demonstrated the involvement of P/Q- and N-type Ca^{2+} channels in the stimulation-induced ACh release in the cardiac parasympathetic postganglionic nerves. These results support the concept that multiple subtypes of the voltage-gated Ca^{2+} channel mediate transmitter release from the same population of parasympathetic neurons (31).

Stimulation-induced ACh release was suppressed by ~50% in the ω-conotoxin GVIA group and by ~80% in the ω-conotoxin MVIIC group. The algebraic summation of the extent of suppression exceeded 100%. The phenomenon may be in part due to the nonlinear dose-response relationship between Ca^{2+} influx and transmitter release (32). The supra-additive phenomenon may be also due to the affinity of ω-conotoxin MVIIC to N-type Ca^{2+} channels (8, 26, 36). Combined local administration of ω-conotoxin GVIA and ω-conotoxin MVIIC almost completely suppressed stimulation-induced ACh release to a level similar to that achieved by the Na^{+} channel inhibitor tetrodotoxin (15). Therefore, involvement of another untested type of Ca^{2+} channel(s) is unlikely in the stimulation-induced ACh release from the cardiac parasympathetic postganglionic nerves in cats.

Ca^{2+} Channels and Ischemia-Induced ACh Release

In a previous study, we showed that acute myocardial ischemia evokes myocardial interstitial ACh release in the ischemic region via a local mechanism independent of efferent vagal nerve activity (14). In that study, the inhibition of intracellular Ca^{2+} mobilization by local administration of 3,4,5-trimethoxybenzoic acid 8-(diethyl amino)-octyl ester (TMB-8) suppressed ischemia-induced ACh release, suggesting that an axoplasmic Ca^{2+} elevation is essential for the ischemia-induced ACh release. Because tissue K^{+} concentration increases in the ischemic region (7, 18), high K^{+}-induced

depolarization could activate voltage-dependent Ca^{2+} channels even in the absence of efferent vagal nerve activity. However, ischemia-induced ACh release was not suppressed by local administration of verapamil, ω-conotoxin GVIA, or ω-conotoxin MVIIC (Fig. 2). Therefore, Ca^{2+} entry through the voltage-dependent Ca^{2+} channels is unlikely a mechanism for the ischemia-induced myocardial interstitial ACh release.

Acute myocardial ischemia causes energy depletion in the ischemic region, which impairs Na^+-K^+-ATPase activity. Ischemia also causes acidosis in the ischemic region, which promotes Na^+/H^+ exchange. As a result, ischemia causes intracellular Na^+ accumulation. The decrease in the Na^+ gradient across the plasma membrane may then cause the Na^+/Ca^{2+} exchanger to operate in the reverse mode, facilitating intracellular Ca^{2+} overload. KB-R7943 can inhibit the reverse mode of Na^+/Ca^{2+} exchange (9, 10) and its potential to protect against ischemia-reperfusion injury has been reported (21). In the present study, however, local administration of KB-R7943 failed to suppress and rather increased ACh release during ischemia as opposed to our expectation. It is plausible that the inhibition of reverse mode of Na^+/Ca^{2+} may have facilitated the accumulation of intracellular Na^+ and induced adverse effects that cancelled the possible beneficial effects derived from the inhibition of Ca^{2+} entry through the Na^+/Ca^{2+} exchanger itself. In addition, KB-R7943 could inhibit the forward mode of Na^+/Ca^{2+} exchange and reduce Ca^{2+} efflux (16), contributing to the intracellular Ca^{2+} accumulation and ACh release. In the present study, we observed the effects of KB-R7943 only during the ischemic period. However, accumulation of intracellular Na^+ through Na^+/H^+ exchange is enhanced on reperfusion due to the washout of extracellular H^+ (20). The inhibition of Na^+/Ca^{2+} exchange to suppress Ca^{2+} overload might become more important during the reperfusion phase. For instance, the percent segment shortening of the left ventricle was improved by KB-R7943 during reperfusion but not during ischemia (35).

As already mentioned, the ischemia-induced ACh release can be blocked by TMB-8 and thus the intracellular Ca^{2+} mobilization is required for the ischemia-induced ACh release (14). Besides the Ca^{2+} entries through voltage-dependent Ca^{2+} channels and via the reverse mode of Na^+/Ca^{2+} exchanger, Ca^{2+} may be mobilized from the endoplasmic reticulum via pathological pathways. As an example, the mitochondrial permeability transition pore triggered in pathological conditions is linked to cytochrome *c* release. Cytochrome *c* can bind to the endoplasmic reticulum Ins(1,4,5)P_3 receptor, rendering the channel insensitive to autoinhibition by high cytosolic Ca^{2+} concentration and resulting in enhanced endoplasmic reticulum Ca^{2+} release (4, 30). In the present study, however, blockade of Ins(1,4,5)P_3 receptor by xestospongin C failed to suppress the ischemia-induced ACh release. In contrast, local administration of gadolinium significantly suppressed the ischemia-induced ACh release. Therefore, nonselective cation channels or cation-selective stretch-activated channels contribute to the ischemia-induced ACh release. During myocardial ischemia, the ischemic region can be subjected to paradoxical systolic bulging. Such bulging likely opens stretch-activated channels and causes myocardial interstitial ACh release, possibly leading to cardioprotection by ACh against ischemic injury (2).

Limitations

First, the experiment was performed under anesthetic conditions, which may have influenced basal autonomic activity. However, because we sectioned the vagi at the neck, basal autonomic activity may have had only a minor effect on ACh release during the vagal stimulation and during acute myocardial ischemia. Second, we added eserine to the perfusate to inhibit immediate degradation of ACh (24), which may have increased the ACh level in the synaptic cleft and activated regulatory pathways such as autoinhibition of ACh release via muscarinic receptors (24). However, the myocardial interstitial ACh level measured under this condition could reflect changes induced by Na^+ channel inhibitor, choline uptake inhibitor, and vesicular ACh transport inhibitor as described in a previous study (15). Therefore, we think that the interpretation of the present results is reasonable. Third, tissue and species differences should be taken into account when extrapolating the present findings, because significant heterogeneity in the Ca^{2+} channels involved in the mammalian parasympathetic system may exist. Finally, we used verapamil to test the involvement of L-type Ca^{2+} channels in the ACh release. There are three major types of L-type Ca^{2+} channel antagonists with different binding domains (verapamil, nifedipine, and diltiazem) (19). Whether the effects on the ACh release are common among the three types of L-type Ca^{2+} channel antagonists remains unanswered.

In conclusion, the N- and P/Q-type Ca^{2+} channels (with the P/Q-type dominant), but probably not the L-type Ca^{2+} channels, are involved in vagal stimulation-induced ACh release from the cardiac parasympathetic postganglionic nerves in cats. In contrast, myocardial interstitial ACh release in the ischemic myocardium is resistant to the blockade of L-, N-, and P/Q-type Ca^{2+} channels. In addition, the ischemia-induced myocardial ACh release is resistant to the inhibition of Na^+/Ca^{2+} exchanger and the blockade of Ins(1,4,5)P_3 receptor but is suppressed by gadolinium, suggesting that nonselective cation channels or cation-selective stretch-activated channels are involved.

GRANTS

This study was supported by Health and Labour Sciences Research Grant for Research on Advanced Medical Technology from the Ministry of Health, Labour and Welfare of Japan, Health and Labour Sciences Research Grant for Research on Medical Devices for Analyzing, Supporting and Substituting the Function of Human Body from the Ministry of Health, Labour and Welfare of Japan, Health and Labour Sciences Research Grant H18-tryo-Ippan-023 from the Ministry of Health, Labour and Welfare of Japan, Program for Promotion of Fundamental Studies in Health Science from the National Institute of Biomedical Innovation, a Grant provided by the Ichiro Kanehara Foundation, Ground-based Research Announcement for Space Utilization promoted by Japan Space Forum, and Industrial Technology Research Grant Program in 03A47075 from New Energy and Industrial Technology Development Organization of Japan.

REFERENCES

1. **Akiyama T, Yamazaki T, and Ninomiya I.** In vivo detection of endogenous acetylcholine release in cat ventricles. *Am J Physiol Heart Circ Physiol* 266: H854–H860, 1994.
2. **Ando M, Katare RG, Kakinuma Y, Zhang D, Yamasaki F, Muramoto K, and Sato T.** Efferent vagal nerve stimulation protects heart against ischemia-induced arrhythmias by preserving connexin43 protein. *Circulation* 112: 164–170, 2005.

3. **Bibevski S and Dunlap ME.** Prevention of diminished parasympathetic control of the heart in experimental heart failure. *Am J Physiol Heart Circ Physiol* 287: H1780–H1785, 2004.
4. **Brookes PS, Yoon Y, Robotham JL, Anders MW, and Sheu SS.** Calcium, ATP, and ROS: a mitochondrial love-hate triangle. *Am J Physiol Cell Physiol* 287: C817–C833, 2004.
5. **Caldwell RA, Clemo HF, and Baumgarten CM.** Using gadolinium to identify stretch-activated channels: technical considerations. *Am J Physiol Cell Physiol* 275: C619–C621, 1998.
6. **Glantz SA.** *Primer of Biostatistics* (5th ed.) New York: McGraw-Hill, 2002.
7. **Hirche HJ, Franz CHR, Bös L, Bissig R, Lang R, and Schramm M.** Myocardial extracellular K^+ and H^+ increase and noradrenaline release as possible cause of early arrhythmias following acute coronary artery occlusion in pigs. *J Mol Cell Cardiol* 12: 579–593, 1979.
8. **Hong SJ and Chang CC.** Calcium channel subtypes for the sympathetic and parasympathetic nerves of guinea-pig atria. *Br J Pharmacol* 116: 1577–1582, 1995.
9. **Iwamoto T, Kita S, Uehara A, Inoue Y, Taniguchi Y, Imanaga I, and Shigekawa M.** Structural domains influencing sensitivity to isothiourea derivative inhibitor KB-R7943 in cardiac Na^+/Ca^{2+} exchanger. *Mol Pharmacol* 59: 524–531, 2001.
10. **Iwamoto T, Watano T, and Shigekawa M.** A novel isothiourea derivative selectively inhibits the reverse mode of Na^+/Ca^{2+} exchange in cells expressing NCX1. *J Biol Chem* 271: 22391–22397, 1996.
11. **Johnson TA, Gray AL, Lauenstein JM, Newton SS, and Massari VJ.** Parasympathetic control of the heart. I. An interventriculo-septal ganglion is the major source of the vagal intracardiac innervation of the ventricles. *J Appl Physiol* 96: 2265–2272, 2004.
12. **Kawada T, Yamazaki T, Akiyama T, Inagaki M, Shishido T, Zheng C, Yanagiya Y, Sugimachi M, and Sunagawa K.** Vagosympathetic interactions in ischemia-induced myocardial norepinephrine and acetylcholine release. *Am J Physiol Heart Circ Physiol* 280: H216–H221, 2001.
13. **Kawada T, Yamazaki T, Akiyama T, Li M, Ariumi H, Mori H, Sunagawa K, and Sugimachi M.** Vagal stimulation suppresses ischemia-induced myocardial interstitial norepinephrine release. *Life Sci* 78: 882–887, 2006.
14. **Kawada T, Yamazaki T, Akiyama T, Sato T, Shishido T, Inagaki M, Takaki H, Sugimachi M, and Sunagawa K.** Differential acetylcholine release mechanisms in the ischemic and non-ischemic myocardium. *J Mol Cell Cardiol* 32: 405–414, 2000.
15. **Kawada T, Yamazaki T, Akiyama T, Shishido T, Inagaki M, Uemura K, Miyamoto T, Sugimachi M, Takaki H, and Sunagawa K.** In vivo assessment of acetylcholine-releasing function at cardiac vagal nerve terminals. *Am J Physiol Heart Circ Physiol* 281: H139–H145, 2001.
16. **Kimura J, Watano T, Kawahara M, Sakai E, and Yatabe J.** Direction-independent block of bi-directional Na^+/Ca^{2+} exchange current by KB-R7943 in guinea-ping cardiac myocytes. *Br J Pharmacol* 128: 969–974, 1999.
17. **Kimura S, Mieno H, Tamaki K, Inoue M, and Chayama K.** Nonselective cation channel as a Ca^{2+} influx pathway in pepsinogen-secreting cells of bullfrog esophagus. *Am J Physiol Gastrointest Liver Physiol* 281: G333–G341, 2001.
18. **Kléber AG.** Extracellular potassium accumulation in acute myocardial ischemia. *J Mol Cell Cardiol* 16: 389–394, 1984.
19. **Kurokawa J, Adachi-Akahane S, and Nagao T.** 1-5-Benzothiazepine binding domain is located on the extracellular side of the cardiac L-type Ca^{2+} channel. *Mol Pharmacol* 51: 262–268, 1997.
20. **Lazdunski M, Frelin C, and Vigne P.** The sodium/hydrogen exchange system in cardiac cells: its biochemical and pharmacological properties and its role in regulating internal concentrations of sodium and internal pH. *J Mol Cell Cardiol* 17: 1029–1042, 1985.
21. **Lee C, Dhalla NS, and Hryshko LV.** Therapeutic potential of novel Na^+-Ca^{2+} exchange inhibitors in attenuating ischemia-reperfusion injury. *Can J Cardiol* 21: 509–516, 2005.
22. **Li M, Zheng C, Sato T, Kawada T, Sugimachi M, and Sunagawa K.** Vagal nerve stimulation markedly improves long-term survival after chronic heart failure in rats. *Circulation* 109: 120–124, 2004.
23. **Molderings GJ, Likungu J, and Göthert M.** N-type calcium channels control sympathetic neurotransmission in human heart atrium. *Circulation* 101: 403–407, 2000.
24. **Nicholls DG.** *Proteins, Transmitters and Synapses*. Oxford: Blackwell Science, 1994.
25. **Oka T, Sato K, Hori M, Ozaki H, and Karaki H.** Xestospongin C, a novel blocker of IP_3 receptor, attenuates the increase in cytosolic calcium level and degranulation that is induced by antigen in RBL-2H3 mast cells. *Br J Pharmacol* 135: 1959–1966, 2002.
26. **Randall A and Tsien RW.** Pharmacological dissection of multiple types of Ca^{2+} channel currents in rat cerebellar granule neurons. *J Neurosci* 15: 2995–3012, 1995.
27. **Schauerte P, Scherlag BJ, Scherlag MA, Goli S, Jackman WM, and Lazzara R.** Ventricular rate control during atrial fibrillation by cardiac parasympathetic nerve stimulation: a transvenous approach. *J Am Coll Cardiol* 34: 2043–2050, 1999.
28. **Serone AP and Angus JA.** Role of N-type calcium channels in autonomic neurotransmission in guinea-pig isolated left atria. *Br J Pharmacol* 127: 927–934, 1999.
29. **Smith AB, Motin L, Lavidis NA, and Adams DJ.** Calcium channels controlling acetylcholine release from preganglionic nerve terminals in rat autonomic ganglia. *Neuroscience* 95: 1121–1127, 2000.
30. **Verkhratsky A and Toescu EC.** Endoplasmic reticulum Ca^{2+} homeostasis and neuronal death. *J Cell Mol Med* 4: 351–361, 2003.
31. **Waterman SA.** Multiple subtypes of voltage-gated calcium channel mediate transmitter release from parasympathetic neurons in the mouse bladder. *J Neurosci* 16: 4155–4161, 1996.
32. **Wheeler DB, Randall A, and Tsien RW.** Changes in action potential duration after reliance of excitatory synaptic transmission on multiple types of Ca^{2+} channels in rat hippocampus. *J Neurosci* 16: 2226–2237, 1996.
33. **Yahagi N, Akiyama T, and Yamazaki T.** Effects of ω-conotoxin GVIA on cardiac sympathetic nerve function. *J Auton Nerv Syst* 68: 43–48, 1998.
34. **Yamazaki T, Akiyama T, Kitagawa H, Takauchi Y, Kawada T, and Sunagawa K.** A new, concise dialysis approach to assessment of cardiac sympathetic nerve terminal abnormalities. *Am J Physiol Heart Circ Physiol* 272: H1182–H1187, 1997.
35. **Yoshitomi O, Akiyama D, Hara T, Cho S, Tomiyasu S, and Sumikawa K.** Cardioprotective effects of KB-R7943, a novel inhibitor of Na^+/Ca^{2+} exchanger, on stunned myocardium in anesthetized dogs. *J Anesth* 19: 124–130, 2005.
36. **Zhang JF, Randall AD, Ellinor PT, Horne WA, Sather WA, Tanabe T, Schwarz TL, and Tsien RW.** Distinctive pharmacology and kinetics of cloned neuronal Ca^{2+} channels and their possible counterparts in mammalian CNS neurons. *Neuropharmacology* 32: 1075–1088, 1993.

Laboratory Investigation

A New Protocol for Quantifying CD34+ Cells

in Peripheral Blood of Patients with Cardiovascular Disease

Akie Kikuchi-Taura
Toshihiro Soma, MD
Tomohiro Matsuyama, MD
David M. Stern, MD
Akihiko Taguchi, MD

Increasing evidence points to a role for circulating CD34-positive (CD34+) cells in vascular maintenance and neovascularization. Although there are established methods for evaluating absolute numbers of CD34+ cells in bone marrow or mobilized peripheral blood, there is no convenient and highly reproducible method for quantifying low numbers of CD34+ cells in blood samples, such as those from the peripheral blood of patients with cardiovascular disease. With current commonly used methods, the mean percentage of CD34+ cells in leukocyte fractions from such patients was only 0.02%, and the cumulative intra-assay coefficient of variation was ~30%. With use of the protocol described herein, actual counts of CD34+ cells increased ~5-fold and cumulative intra-assay coefficients of variation were reduced to ~7%. The new method is useful to precisely measure low numbers of CD34+ cells in samples, and it has potential as a screening tool to evaluate cardiovascular risk in large patient populations. ***(Tex Heart Inst J 2006;33:427-9)***

Key words: *Antigens, CD34/analysis; blood cell count; cardiovascular diseases; cell sorter, fluorescence-activated; CD34-positive cells; coefficients of variation; endothelium, vascular/cytology; stem cells*

From: *Department of Clinical Laboratory (Ms Kikuchi-Taura and Dr. Soma), National Hospital Organization, Osaka Minami Medical Center, Osaka 586-8521, Japan; Department of Internal Medicine (Dr. Matsuyama), Hyogo College of Medicine, Hyogo 663-8501, Japan; College of Medicine (Dr. Stern), University of Cincinnati, Cincinnati, Ohio 45221; and Department of Cerebrovascular Disease (Dr. Taguchi), National Cardiovascular Center, Osaka 565-8565, Japan*

This work was supported by a Grant-in-Aid for Scientific Research from the Ministry of Health, Labor, and Welfare, Japan.

Address for reprints: *Akihiko Taguchi, MD, Department of Cerebrovascular Disease, National Cardiovascular Center, 5-7-1 Fujishiro-dai, Suita, Osaka 565-8565, Japan*

E-mail: ataguchi@res.ncvc.go.jp

© 2006 by the Texas Heart® Institute, Houston

In vasculature maintenance and neovascularization, there is increasing evidence of a role for circulating endothelial progenitor cells (EPCs)—including the populations of CD34-positive (CD34+) cells that are present in peripheral blood.[1] As a source of numerous growth and angiogenesis factors at ischemic loci, CD34+ cells also contribute to vascular homeostasis.[2] Furthermore, initial clinical trials of cell transplantation in treating ischemia of the hind limb[3] and myocardium[4] have shown promising results. On the basis of these observations, circulating EPCs[5] and CD34+ cells[6] have been evaluated in patients with cardiovascular disease, and strong correlations of their levels with vascular function have been reported. However, procedures to evaluate EPCs and CD34+ cells are not simple[5]; because of low numbers of circulating CD34+ cells, routine FACS (fluorescence-activated cell sorter) analysis[7] of CD34+ cell counts in patients with cardiovascular disease is not feasible. In this report, we demonstrate a new method that facilitates determination of the absolute number of circulating CD34+ cells in patients with low levels of CD34+ cells.

Patients and Methods

This study was approved by the Human Assurance Committee of the National Cardiovascular Center and Osaka Minami Medical Center, and all subjects provided written informed consent. Results of experiments are reported as mean ± standard error.

Analysis of Peripheral Blood

Three milliliters of heparinized peripheral blood were obtained from 20 patients who had histories of cardiovascular disease: 14 had sustained myocardial infarction, and 9 had sustained cerebral infarction (3 had histories of both). Patients who had experienced vascular events within 30 days of measurement were excluded. The study group included 12 men and 8 women, with a mean age of 74 ± 1.7 years (range, 59–87 yr). Medicines taken by study subjects included anticoagulants (aspirin, 17); antihypertensive agents, including calcium-channel antagonists, angiotensin-converting enzyme (ACE) inhibitors, or both (14); and sulfonylureas for glycemic control (5). Patients who were taking HMG-CoA reductase inhibitors (statins) were excluded from the study.

First, we counted circulating CD34+ cells with ProCount™ (BD Bioscience; San Jose, Calif) and Stem-Kit™ (Beckman Coulter; Marseilles, France), according to the

TABLE I. Reduction in the Coefficient of Variation Using Our Modified, Improved Protocol for Determining CD34+ Cell Levels in Peripheral Blood

	ProCount	Stem-Kit	Improved Protocol
Actual CD34+ cell counts Range	16 ± 1 10–31	34 ± 4 16–58	174 ± 18 88–404
CD34+ cells in leukocytes (%) Range	0.024 ± 0.003 0.012–0.046	0.021 ± 0.001 0.011–0.032	0.019 ± 0.002 0.014–0.038
Circulating CD34+ cells (cells/μL)	0.82 ± 0.05	0.81 ± 0.06	0.88 ± 0.06
Cumulative intra-assay coefficient of variation (%)	30.3	25.7	7.4

ments using the standard method (Table I). The supernatant that was removed during the procedure was also analyzed and was found not to contain either cells or internal control particles.

Improvement in the Cumulative Intra-Assay Coefficient of Variation

In mobilized peripheral blood, the coefficients of variation have been reported to be about 8% and 4% using ProCount and Stem-Kit, respectively, on the basis of the manufacturers' published information. However, in non-mobilized peripheral blood of patients with cardiovascular disease, the mean percentage of $CD34^+$ cells in the leukocyte fraction was less than 10%, compared with mobilized blood, and the calculated cumulative intra-assay coefficients of variation were 30.3% and 25.7%, as evaluated by ProCount and Stem-Kit, respectively. Our method increased the absolute number of $CD34^+$ cells by about 5-fold during the same measurement period, and it resulted in a reduced (7.4%) cumulative intra-assay coefficient of variation (Table I).

Discussion

Although our modified method for quantifying $CD34^+$ cells in blood was similar to established methods for the calculation of mean circulating $CD34^+$ cell counts, our method substantially improved reproducibility of the measurement.

The coefficient of variation of $CD34^+$ cell counts is inversely proportional to the square root of the number of $CD34^+$ cells detected in the sample. A minimum of 100 $CD34^+$ cells is required to ensure a coefficient of variation in the range of 10%.[8] Our modified protocol yielded more than 100 $CD34^+$ cells in each count (confirmed by duplicate counting), and the coefficient of variation was reduced to 7%. Simply increasing the sample volume or lengthening the time for measurement of cell numbers does not necessarily improve reproducibility of the counts.[8] Our results indicate that absolute numbers of circulating $CD34^+$ cells in peripheral blood of patients who have low levels of such cells can now be quantified precisely using a modification of the ISHAGE protocol. This easy method enables precise measurement of the $CD34^+$ cell population of stem cells in peripheral blood and can be broadly applied to screening patients for cardiovascular risk.

References

1. Asahara T, Murohara T, Sullivan A, Silver M, van der Zee R, Li T, et al. Isolation of putative progenitor endothelial cells for angiogenesis. Science 1997;275:964-7.
2. Majka M, Janowska-Wieczorek A, Ratajczak J, Ehrenman K, Pietrzkowski Z, Kowalska MA, et al. Numerous growth factors, cytokines, and chemokines are secreted by human CD34(+) cells, myeloblasts, erythroblasts, and megakaryoblasts and regulate normal hematopoiesis in an autocrine/paracrine manner. Blood 2001;97:3075-85.
3. Taguchi A, Ohtani M, Soma T, Watanabe M, Kinosita N. Therapeutic angiogenesis by autologous bone-marrow transplantation in a general hospital setting. Eur J Vasc Endovasc Surg 2003;25:276-8.
4. Hamano K, Nishida M, Hirata K, Mikamo A, Li TS, Harada M, et al. Local implantation of autologous bone marrow cells for therapeutic angiogenesis in patients with ischemic heart disease: clinical trial and preliminary results. Jpn Circ J 2001;65:845-7.
5. Hill JM, Zalos G, Halcox JP, Schenke WH, Waclawiw MA, Quyyumi AA, Finkel T. Circulating endothelial progenitor cells, vascular function, and cardiovascular risk. N Engl J Med 2003;348:593-600.
6. Taguchi A, Matsuyama T, Moriwaki H, Hayashi T, Hayashida K, Nagatsuka K, et al. Circulating CD34-positive cells provide an index of cerebrovascular function. Circulation 2004;109:2972-5.
7. Sutherland DR, Anderson L, Keeney M, Nayar R, Chin-Yee I. The ISHAGE guidelines for CD34+ cell determination by flow cytometry. International Society of Hematotherapy and Graft Engineering. J Hematother 1996;5:213-26.
8. Sutherland DR, Keeney M, Gratama JW. Enumeration of CD34+ hematopoietic stem and progenitor cells. In: Robinson JP, Darzynkiewicz Z, Dobrucki J, Hyun WC, Nolan JP, Orfao A, Rabinovitch PS, editors. Current protocols in cytometry. New York: John Wiley and Sons, Inc.; 2003. Unit 6.4, p. 1-23.

manufacturers' protocols. (These protocols are based on International Society of Hematotherapy and Graft Engineering (ISHAGE) Guidelines[7] and are frequently used for quantification of CD34+ cells that have mobilized into peripheral blood.) Next, to increase the reproducibility of CD34+ cell counts, the Stem-Kit protocol was modified as follows: the blood sample volume, antibodies, and lysing solution were doubled. After adding 30 µL of internal control particles (stem count: Beckman Coulter), samples were centrifuged for 5 min at 450 G, and 3,860 µL of supernatant was removed carefully with a pipette. Samples were analyzed by Coulter CYTOMICS™ FC500 & XL-system II software (Beckman Coulter) for 6 min each (Fig. 1).

Results

Increase of CD34+ Cell Counts

The mean percentage of CD34+ cells in the leukocyte fraction obtained from mobilized peripheral blood has been reported to be about 0.2% to 0.5%.[7] First, we used the ProCount and Stem-Kit protocols to count circulating CD34+ cells that had been obtained from patients with cardiovascular disease (Table I). The mean percentages of CD34+ cells in the leukocyte fraction were 0.024% ± 0.003% (range, 0.012%–0.046%) for ProCount and 0.021% ± 0.001% (range, 0.011%–0.032%) for Stem-Kit. The actual CD34+ cell counts per analysis were only 16 ± 1 (range, 10–31) for ProCount and 34 ± 4 (range, 16–58) for Stem-Kit. Because the absolute cell count is a major factor in the reproducibility of the measurement,[8] our approach was to modify the original protocol in order to obtain higher numbers of actual CD34+ cells per count. However, simply increasing sample volume or measurement time does not improve reproducibility, because of these factors: adhesion of internal control particles to cells in the patient sample, and precipitation and aggregation of cells in the sample. Our approach, as outlined under Methods, was to seek a method that produces higher cell counts while maintaining short measurement times. Through the use of our method, the mean CD34+ cell count increased to a level of 174 ± 18 (range, 88–404) per analysis, and the mean percentage of CD34+ cells in the leukocyte fraction was 0.019 ± 0.002 (range, 0.014%–0.038%), which was consistent with measure-

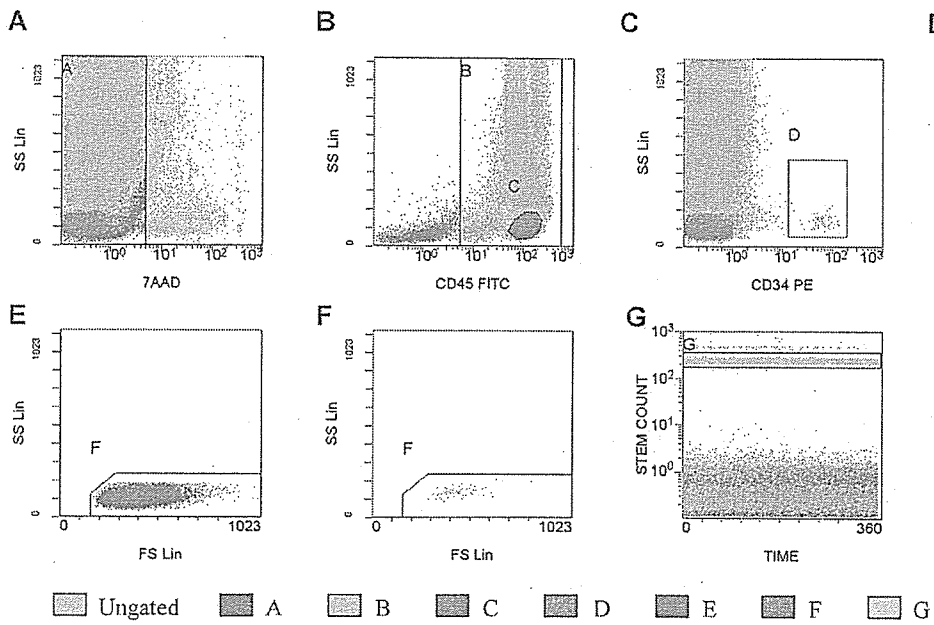

Fig. 1 *Quantification of circulating CD34+ cells by fluorescence-activated cell sorter analysis using our modified, improved protocol.* ***A)*** *All events: 7-aminoactinomycin-D viability dye-positive cells (dead cells) were excluded from region A.* ***B)*** *Events from region A: All CD45+ cells (leukocytes) were included in region B. Region C was adjusted to include only lymphocytes (bright CD45, low side-scatter).* ***C)*** *Events from regions A and B: Region D was adjusted to include CD34+ hematopoietic progenitor cells (HPC).* ***D*** *Events from regions A, B, and D: Region E was adjusted to include cells forming a cluster with characteristic CD34+ HPC (low side-scatter and low-to-intermediate CD45 staining). Brightly stained events were excluded from region E.* ***E)*** *Events from regions A and C: Region F was adjusted to include lymph/blast cells, excluding platelet aggregates if present.* ***F)*** *Events from A, B, D, and E: Lymph/blast region F identified a cluster of events that met all the fluorescence and light-scattering criteria of ISHAGE Guidelines for CD34+ HPC.* ***G)*** *All events: Region G was adjusted to enclose the internal control.*

7AAD = 7-aminoactinomycin-D; CD34 PE = cluster of differentiation 34 phycoerythrin; CD45 FITC = cluster of differentiation 45 fluorescein isothiocyanate; FS Lin = forward-scatter linear scale; ISHAGE = International Society of Hematotherapy and Graft Engineering; SS Lin = side-scatter linear scale

Biphasic Action of Inducible Nitric Oxide Synthase in a Hindlimb Ischemia Model

Koji Kimura[1], Takako Goto[1], Kentarou Yagi[1], Hidekazu Furuya[1], Shio Jujo[2], Johbu Itoh[3], Sadaaki Sawamura[4], Shirosaku Koide[1], Hidezo Mori[5,*], and Naoto Fukuyama[2,*]

[1]Department of Surgery, Division of Cardiovascular Surgery, School of Medicine, Tokai University, Kanagawa 259-1193, Japan
[2]Department of Physiology School of Medicine, Tokai University, Kanagawa 259-1193, Japan
[3]Department of Pathology School of Medicine, Tokai University, Kanagawa 259-1193, Japan
[4]Department of Microbiology, School of Medicine, Tokai University, Kanagawa 259-1193, Japan
[5]Department of Cardiac Physiology, National Cardiovascular Center, Osaka 565-8565, Japan

Received 17 October, 2005; Accepted 22 November, 2005

Summary **We investigated the influence of inducible nitric oxide synthase (iNOS) on acute ischemic injury and chronic angiogenesis. In a hindlimb ischemia model, NO produced by endothelial NO synthase (eNOS) reduces ischemic injury and promotes angiogenesis. However, the effect of the large amounts of NO generated by induced iNOS is unclear. Experimental groups of mice were as follows: (1) wild-type group (Wild), (2) iNOS-knockout group (iNOS-KO), and (3) aminoguanidine-treated wild-type group (Wild + AG), which received aminoguanidine from day 0 to day 3 after ischemia. Acute ischemic injury was evaluated by measuring the plasma CK value and ischemic score. Chronic angiogenesis was evaluated by microangiography and with a non-contact type Doppler blood flowmeter on day 3. Compared with the Wild group (251 ± 34.7 IU/l), the CK value was significantly elevated in the iNOS-KO (497 ± 126.7 IU/l) and Wild + AG (587.2 ± 128.7 IU/l) groups. The ischemic score was significantly increased in the iNOS-KO (92%) and Wild ± AG (66.6%) groups compared with the Wild group (23%). Blood flow was significantly increased in the iNOS-KO group (58.7 ± 15.3%) compared with the Wild (38.1 ± 15.9%) and Wild ± AG (43.5 ± 9.8%) groups in the chronic stage. Microangiography revealed a significantly increased number of blood vessels in the iNOS-KO (0.29 ± 0.02) group compared with the Wild (0.12 ± 0.01) and Wild + AG (0.15 ± 0.02) groups. Our findings indicate that NO generated by iNOS has a biphasic action, reducing acute ischemic injury and inhibiting angiogenesis in the chronic stage.**

Key Words: **angiogenesis, ischemia, nitric oxide synthase**

Introduction

The incidence of refractory peripheral arterial disease is increasing rapidly in developed countries [*1*]. When peripheral arterial disease becomes severe, not only is the quality of life of patients impaired, but also their prognosis is poor [*2*]. Consequently new therapies, including angiogenic treatment with vascular endothelial growth factor (VEGF), hepatocyte growth factor (HGF) and fibroblast growth factor-4 (FGF-4) gene transduction or bone marrow cells, have been developed, with some success [*3-8*].

NO is produced by NO synthase and has multiple bioactivities, including vasodilating, anti-platelet-aggregating

*To whom correspondence should be addressed.
Tel: +81-463-931-121 Fax: +81-463-936-684
E-mail: fukuyama@is.icc.u-tokai.ac.jp

and anti-microbial activities [*9*]. Among the three NO synthase isoforms, neuronal NO synthase (nNOS) is found in the central nerve system, and iNOS is induced in smooth-muscle cells and inflammatory cells in various diseases, such as endotoxemia or ischemia, while eNOS is found in vascular endothelial cells [*10*].

NO generally has a cytoprotective action on hindlimb ischemia [*11–14*]. During ischemic injury, eNOS is upregulated and iNOS is induced. It is reasonable that NO produced by eNOS reduces acute ischemic injury and induces angiogenesis, as it has been shown to have a vasodilatory action [*15–17*]. Induced iNOS produces large amounts of NO [*18*], but the effect of NO generated by iNOS in hindlimb ischemia remains unclear.

In this experiment, we examined the contributions of iNOS to the acute phase of ischemic injury and to angiogenesis in the chronic phase of ischemia in a mouse hindlimb ischemia model, using iNOS knockout mice and wild-type mice treated with aminoguanidine (a selective inhibitor of inducible nitric oxide synthese in macrophages)[*19–21*] in the acute phase.

Materials and Methods

Mice

All mice used in experiments were male, 2 to 3 months of age, weighing 18 to 26 g each. Wild-type (Wild) 129 SvEv mice were purchased from CLEA, Japan. iNOS –/– mice, with a mixed C57BL/6J × 129 SvEv genetic background, were obtained from Merck & Co, Inc.. INOS +/+ mice were obtained by crossing 129 SvEv mice with C57BL/6J mice twice. INOS –/– and iNOS +/+ strains have similar genetic backgrounds of 75% C57BL/6J and 25% 129/SvEv [*22*]. For the pharmacologically iNOS-inhibited group, Wild mice were given aminoguanidine (AG; Sigma, 50 mg/kg, i.p., KI value of 55 micro M and a $K_{inact\ max}$ value of 0.09 min^{-1}) [*23*] 24 hr before operation and daily for 3 days postoperatively [*24, 25*]. The animals were maintained in a pathogen-free barrier facility with a 12-hour light/dark cycle and had free access to food and water. Animals were anesthetized with pentobarbital sodium (50 mg/kg, i.p.), and hindlimb ischemia was created by ligation of the left common iliac artery and external iliac artery and resection of the femoral artery [*26, 27*]. Mice were killed 7 days (acute phase) or 14 to 21 days (chronic phase) after surgery [*28*]. The study was approved by the Animal Care Committee of Tokai University.

Evaluation of acute ischemic injury

Serum CK value—To estimate skeletal muscle injury, CK release was estimated in the effluent collected from the infraorbitalis vein on day 3. Plasma was obtained through centrifugation of the whole blood for 10 minutes at 12000 g at 4°C. Plasma was collected and CK was assayed by SRL Co..

Ischemic score—On day 7, the degree of ischemic insult in the limb was macroscopically evaluated by using graded morphological scales for tissue necrosis (grade 0 to IV): grade 0: absence of necrosis: grade I, necrosis only of toes; grade II, necrosis extending to dorsum of a foot; grade III, necrosis extending to crus; grade IV, necrosis extending to a thigh or complete necrosis (Fig. 1).

Evaluation of chronic angiogenesis

Non-contact type laser Doppler measurement—We employed laser Doppler flowmetry (LDF), a non-nvasive technique for measuring tissue blood flow [*16, 29*], using a FLO-N1 device (OMEGAWAVE, Japan), which delivers light generated by a semiconductor laser diode operating at a wavelength of 780 nm, with a maximum accessible power of 3 mW. Briefly, the skin was removed so that only deep muscle blood flow would be measured, and the probe (ST-N probe, OMEGAWAVE, Japan) was placed on 4 points of the femoral muscles. Blood flow was expressed as ml/min/100 g. The contralateral hindlimb served as an internal control.

Sequential microangiography in in vivo—A PE-10 (10-gauge polyethylene) catheter was placed in the right common carotid artery of a mouse fixed on a board (1.0 mm thick) in the standing position under general anesthesia. Sequential images of the hind limb were obtained by the injection of non-ionic contrast material (1 ml/s for 2 s, Iopamidol, Nihon Schering, Tokyo, Japan) via the arterial catheter [*30*] on day 0 and day 14. Monochromatic synchrotron radiation with an energy level of 33.3 keV was obtained with a silicon crystal from beamlines NE5 and BL-14 at the High Energy Accelerator Research Organization, Tsukuba, Japan. To improve contrast resolution, subtraction images were created in the computer from the digital images obtained immediately before and during contrast material injection [*31*]. Angiogenesis was evaluated in terms of vessel density and assigned an angiographic score [*28, 32, 33*]. The ischemic signal in the acute phase is a critical factor inducing angiogenesis [*34*], and angiogenesis increases in proportion to the degree of ischemia [*35, 36*]. Therefore, angiogenesis should be compared among groups with comparable severity of acute ischemic injury. For this reason, we compared results among groups using only animals with grade I ischemic score (refer to Figure 3).

FITC gel angiography—To visualize microvessel networks, the FITC-gelatin conjugate fluorescence injection method (dialyzed FITC, 30 mg/mL conjugated gelatin solution) was employed [*37*]. Mice were anesthetized with pentobarbital sodium (50 mg/kg, i.p.), and a PE-10 (10-gauge polyethylene) catheter was placed in the right common carotid artery. The FITC gelatin solution (20 ml) was injected into the catheter

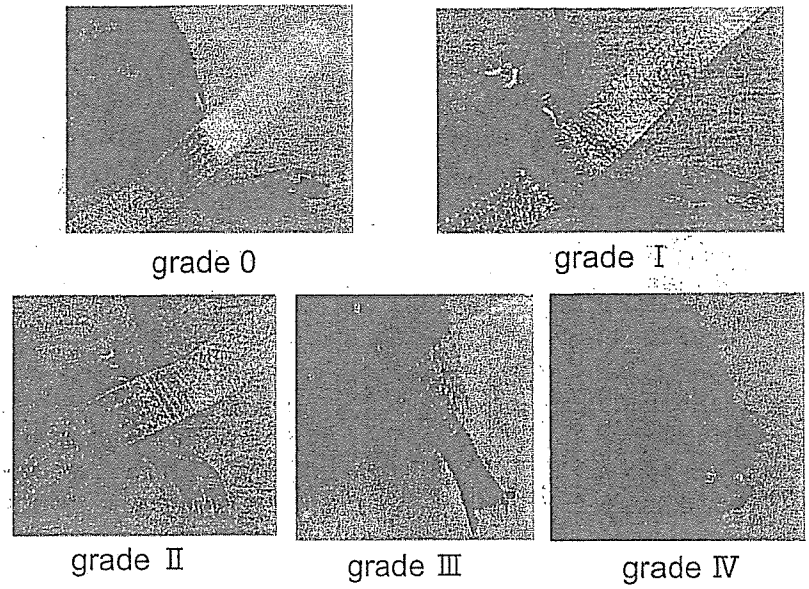

grade	necrotic area
0	none
I	only toes
II	extending to dorsum pedis
III	extending to crus
IV	extending to thigh or complete necrosis

Fig. 1. The grading of necrosis in ischemic hindlimb. The ischemic limb was macroscopically evaluated by using a graded morphological scale for tissue necrosis area (grade 0 to IV).

(1 ml/min) and the right common carotid vein was cut. After complete perfusion, the left leg were resected and immediately fixed in ice-cold graded paraformaldehyde (4%). A confocal laser scanning microscopy (CLSM) system (LSM-410, Carl Zeiss, Jena, Germany), equipped with a 488-nm argon laser (for FITC), was employed on thick sections (1–2 mm) to visualize microvessel networks in detail [*38*]. After computer-assisted 3-D imaging of microvessel networks by the CLSM system, the images were stored on hard disk memory or a magnetic optical disk, EDM-230C (Sony, Tokyo, Japan) and were printed with a digital Pictrostat 400 (Fuji Film Co/Ltd., Tokyo, Japan).

Statistical Analysis

Data are presented as mean values ± SD. Differences were assessed by using one-way ANOVA with Tukey's post test.

Results

Acute ischemic injury

Serum CK value—Firstly, we measured serum CK value to evaluate the acute ischemic injury in the three experimental groups. In the control (Wild) group, the serum CK value was 251 ± 34.7 IU/l. The serum CK values in the Wild + AG group (587.2 ± 128.7 IU/l) and iNOS-KO group (497 ± 126.7 IU/l) were significantly higher than that in the Wild group (Figure 2).

Ischemic score on day 7—The ischemic scores in the iNOS-KO group (92%) and the Wild + AG group (66.6%) were significantly higher than that in the Wild group (23%) (Figure 3). Percentages of grade I in the Wild, iNOS-KO and Wild + AG groups were 23%, 25% and 33%, respectively.

Chronic angiogenesis

Laser Doppler (non contact type) measurement—The

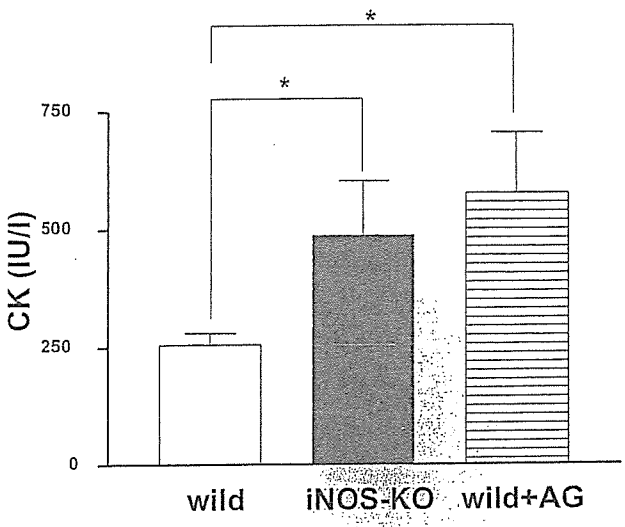

Fig. 2. Serum CK value in acute hindlimb ischemia. Open bar, control group; closed bar, iNOS-knockout (iNOS-KO) group; hatched bar, aminoguanidine-treated group (Wild + AG). The CK values in the iNOS-KO group and Wild + AG group were significantly higher than that in the control (Wild) group (*p<0.05).

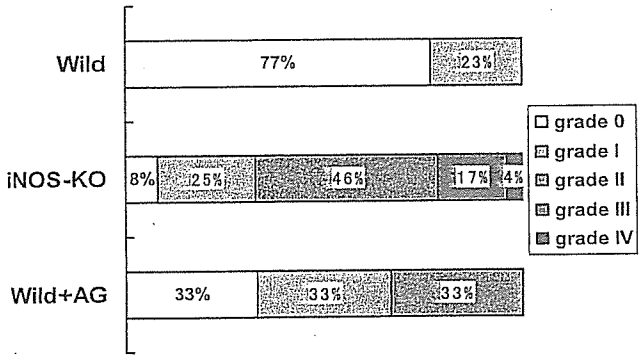

Fig. 3. Ischemic score in acute hindlimb ischemia. Open column, grade 0; dotted column, grade I; vertically lined column, grade II; hatched column, grade III; cross lined column, grade IV.

blood flow at the ischemic lesion was significantly reduced in all three groups on day 3 after surgery. However, at post-operative day 14, it was significantly higher in the iNOS-KO group (58.7 ± 8.7%) than in the Wild group (38.1 ± 5.2%) or the Wild + AG group (43.5 ± 6.4%) (Figure 4).

Sequential microangiography in in vivo—No vessels were apparent in hind limb angiography on day 0, and fine vessels were barely visible on day 14 in the Wild group (Figure 5 A and B). In contrast, many vessels were supplying the hind-limb on the injured side on day 14 in the iNOS-KO group. The angiogenic score on day 14 was significantly increased in the iNOS-KO group (0.29 ± 0.02) compared with that in

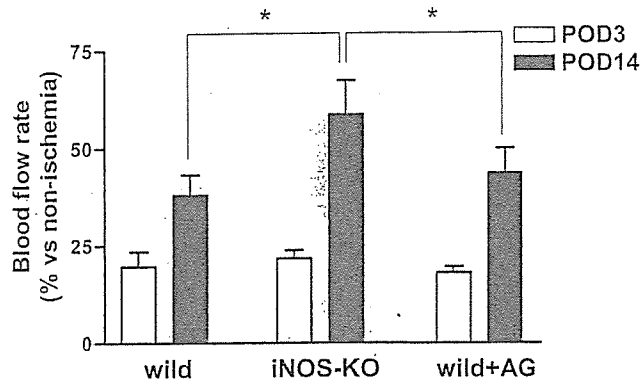

Fig. 4. Blood flow rate in non-contact laser-Doppler flowmetry. Open bar, blood flow ratio on day 3. Closed bar, blood flow ratio on day 14. The blood flow ratio on day 14 in the iNOS-KO group was significantly higher than in the Wild group or Wild + AG group (*p<0.05).

the Wild group or the Wild + AG group (0.12 ± 0.01 and 0.15 ± 0.02, respectively) (p<0.05) (Figure 5).

FITC angiography—The presence of fine vascular networks in the iNOS-KO group (Fig. 6B) implies that marked angiogenesis had occurred. There was a distinct difference in induction of vascular networks between the iNOS-KO group and the Wild and Wild + AG groups (Figure 6 A,B,C).

Discussion

In this experiment, ischemic injury was severe, but angiogenesis was markedly greater in the iNOS-KO group than in the Wild + AG or Wild group. The results indicate that NO generated by iNOS inhibited acute ischemic injury, but reduced angiogenesis in the chronic stage of ischemia.

Of the three NO synthese isoforms, nNOS is mainly localized in the central nervous system, postsynaptic density (PSD), and muscular sarcolemma (muscle fiber myelin) and participates in neural transmission [*39-41*]. iNOS is usually not expressed, but is induced in vascular smooth muscle cells and macrophages *via* cytokine stimulation during sepsis or ischemia with or without reperfusion, and produces large quantities of NO [*42*]. eNOS is mainly localized in vascular endothelial cells and produces NO continuously in response to shear stress, playing important roles in platelet aggregation and vasodilation [*12, 17*]. So, it appears reasonable that NO inhibits acute ischemic injury. In contrast, many studies have shown that NO production by iNOS aggravates injury in the hindlimb ischemia model. Nevertheless, we found that iNOS reduced ischemic injury in the acute stage in the present experiment. A key difference between our study and the others is the presence or absence of reperfusion following the ischemic period. We have

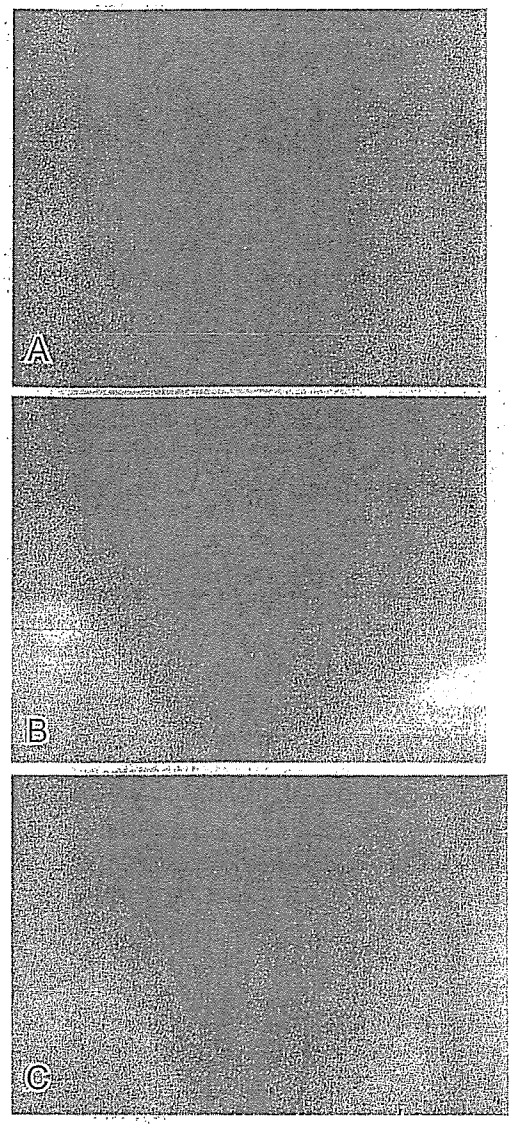

Fig. 5. Representative microangiograms. A : angiogram taken on day 0 in an animal of the Wild group ; B : angiogram taken on day 14 in an animal of the Wild group ; C : angiogram taken on day 14 in an animal of the iNOS-KO group.

already reported that superoxide ($O_2^{\cdot-}$) is produced in ischemic tissue at the time of reperfusion, and reacts with NO to form peroxynitrite [*43*]. Peroxynitrite is a potent oxidant that directly oxidizes sulfhydryl groups at a 1000-fold greater rate than hydrogen peroxide. It inhibits the function of various enzymes, including components of the mitochondrial electron transport chain. In our experiment, we examined ischemia without reperfusion, so that $O_2^{\cdot-}$ (and hence peroxynitrite) would not be produced, and only NO was present.

A second difference from previous experiments is that we used mice treated with iNOS inhibitor in the acute stage, as well as iNOS knockout mice, to examine the effect of iNOS [*44*]. It is noteworthy that one study in which iNOS knockout mice were used and reperfusion was not performed (similar to our protocol) found that injury was severe and angiogenesis in the chronic stage was augmented [*45*]. This is consistent with our results, and indicates that reperfusion plays a critical role in the outcome [*46*].

As the ischemic signal in the acute phase is a critical factor inducing angiogenesis [*34*], and angiogenesis increases in proportion to the degree of ischemia [*35, 36*], angiogenesis has to be compared among groups with comparable severity of acute ischemic injury. We therefore selected animals with grade I ischemic score in all cases for comparison among groups. Aminoguanidine was administered for only three days in the Wild + AG group in order to allow iNOS to function in the chronic stage. At corresponding levels of acute ischemia, angiogenesis in the chronic stage was obviously enhanced in the iNOS-KO group in comparison with the Wild + AG group, i.e., angiogenesis in the chronic stage was inhibited by the function of iNOS.

Many reports indicate that iNOS enhances angiogenesis in various neoplastic disease models [*44, 47–49*]. However, factors secreted by the cancer cells may play important roles in these models. It is important to note that our results showing a biphasic action of iNOS depended on the use of both an acutely iNOS inhibitor-treated wild-type group and an iNOS knockout group in an ischemic model. The mechanism underlying the inhibitory action of NO appears to be down-regulation of the VEGF receptor [*50*]. Possible compensatory roles of eNOS and nNOS in iNOS knockout mice have been ruled out by a previous study, in which their expression was shown to remain unchanged [*51*].

In summary, we have shown that iNOS reduces acute ischemia, but inhibits angiogenesis in a hindlimb ischemia model. Thus we suggest to use iNOS inducer or agents to increase NO production such as arginine with acute phase and supplement iNOS inhibitor in chronic stage. However these remained to be examined prior to clinical trial.

Acknowledgment

This work was supported by grants from Tokai University School of Medicine Research Aid in 2004, the research and study program of Tokai University Educational System General Research Organization and Kanagawa Nanbyou Foundation in 2004, as well as a Grant-in-Aid for Scientific Research in 2003 (No. 15659285) from the Ministry of Education, Science and Culture, Japan and Health and Labour Sciences Research Grants for Research on Human Genome, Tissue Engineering Food Biotechnology in 2003 (H15-saisei-003).

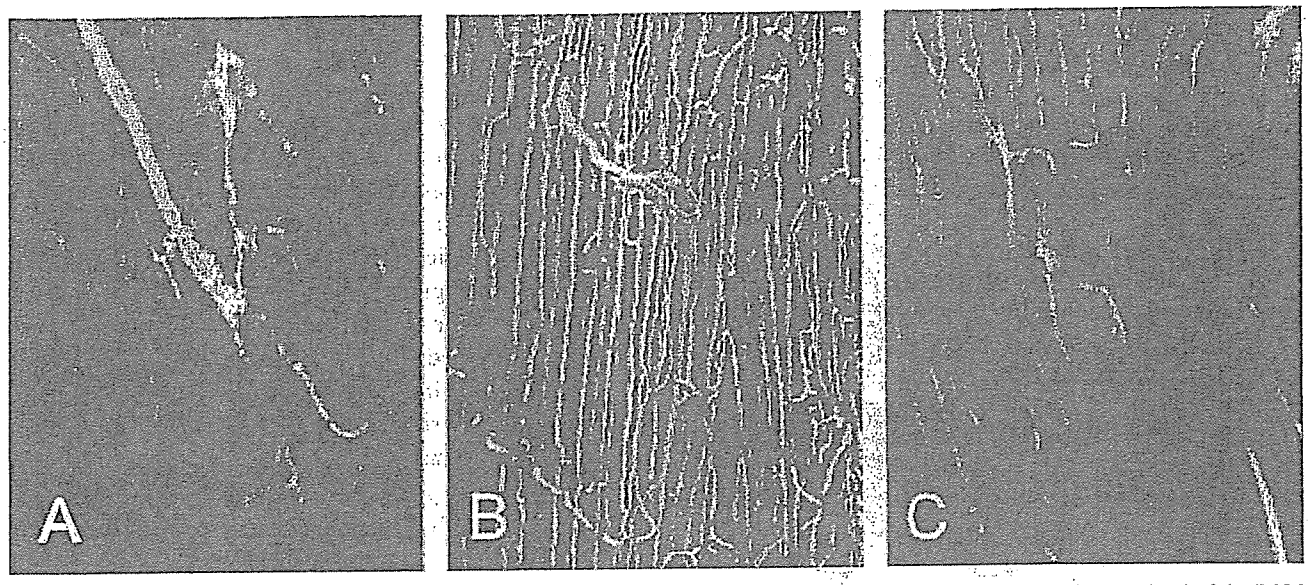

Fig. 6. FITC angiography. FITC angiograms were evaluated on day 14. A: in an animal of the Wild group; B: in an animal of the iNOS-KO group; C: in an animal of the Wild + AG group. Clear angiogenesis was visualized in the iNOS-KO group compared with the control group and aminoguanidine-treated group.

References

[1] Rosamond, W.D., Chambless, L.E., Folsom, A.R., Cooper, L.S., Conwill, D.E., Clegg, L., Wang, C.H., and Heiss, G.: Trends in the incidence of myocardial infarction and in mortality due to coronary heart disease, 1987 to 1994. *N. Engl. J. Med.*, **339**, 861-867, 1998.

[2] Mukherjee, D., Bhatt, D.L., Roe, M.T., Patel, V., and Ellis, S.G.: Direct myocardial revascularization and angiogenesis-How many patients might be eligible? *Am. J. Cardiology.*, **84**, 598-600, 1999.

[3] Isner, J.M. and Asahara, T.: Angiogenesis and vasculogenesis as therapeutic strategies for postnatal neovascularization. *J. Clin. Invest.*, **103**, 1231-1236, 1999.

[4] Carmeliet, P., Ng, Y.S., Nuyens, D., Theilmeier, G., Brusselmans, K., Cornelissen, I., Ehler, E., Kakkar, V.V., Stalmans, I., Mattot, V., Perriard, J.C., Dewerchin, M., Flameng, W., Nagy, A., Lupu, F., Moons, L., Collen, D., Amore, P.A.D., and Shima, D.T.: Impaired myocardial angiogenesis and ischemic cardiomyopathy in mice lacking the vascular endothelial growth factor isoforms $VEGF_{164}$ and $VEGF_{188}$. *Nature. Med.*, **5**, 495-502, 1999.

[5] Jayasnkar V., Woo J., Bish L.T., Pirolli T.J., Chatterjee S., Berry M.F., Burdick J., Gardner T.J., and Sweeney H.L.: Gene transfer of hepatocyte growth factor attenuates postinfarction heart failure. *Circulation*, **108**[suppl II], II-230-II-236, 2003.

[6] Taniyama, Y., Morishita, R., Hiraoka, K., Aoki, M., Nakagami, H., Yamasaki, K., Matsumoto, K., Nakamura, T., Kaneda, Y., and Ogihara,T.: Therapeutic angiogenesis induced by human hepatocyte growth factor gene in rat diabetic hind limb ischemia model. Molecular mechanisms of delayed angiogenesis in diabetes. *Circulation*, **104**, 2344-2350, 2001.

[7] Grines, C.L., Watkins, M.W., Helmer, G., Penny, W., Brinker, J., Marmur, J.D., West, A., Rade, J.J., Marrott, P., Hammond, H.K. and Engler, R.L.: Angiogenic gene therapy (AGENT) trial in patients with stable angina pectoris. *Circulation*, **105**, 1291-1297, 2002.

[8] Tateishi-Yuyama, E., Matsubara, H., Murohara, T., Ikeda, U., Shintani, S., Masaki, H., Amano, K., Kishimoto, Y., Yoshimoto, K., Akashi, H., Shimada, K., Iwasaka, T., and Imaizumi, T.: Therapeutic angiogenesis for patients with limb ischemia by autologous transplantation of bone-marrow cells: a pilot study and a randomized controlled trial. *Lancet*, **360**, 427-435, 2002.

[9] Randomski, M.W., Vallance, P., Whitley, G., Foxwell, N., and Moncada, S.: Platelet adhesion to human vascular endothelium is modulated by constitutive and cytokine induced nitric oxide. *Cardiovasc. Res.*, **27**, 1380-1382, 1993.

[10] Förstermann, U., Closs, E.I., Pollock, J.S., Nakane, M., Schwarz, P., Gath, I., and Kleinert, H.: Nitric oxide synthase isozymes characterization, molecular cloning, and functions. *Hypertension*, **23**, 1121-1131, 1994.

[11] Ziche, M., Morbidelli, L., Masini, E., Amerini, S., Granger, H.J., Maggi, C.A., Geppetti, P., and Ledda, F.: Nitric Oxide Mediates Angiogenesis *in vivo* and endothelial cell growth and migration *in vitro* promoted by substance P. *J. Clin. Invest.*, **94**, 2036-2044, 1994.

[12] Papapetropoulos, A., Desai, K.M., Rudic, R.D., Mayer, B., Zhang, R., Ruiz-Torres, M.P., García-Cardeña, G., Madri, J.A., and Sessa, W.C.: Nitric oxide synthase inhibitors attenuate transforming-growth-factor-β_1-stimulated capillary organization *in vitro*. *Am. J. pathol.*, **150**, 1835-1844, 1997.

[13] Ziche, M., Morbidelli, L., Choudhuri, R., Zhang, H.T., Donnini, S., Granger, H.J., and Bicknell, R.: Nitric oxide

synthase lies downstream from vascular endothelial growth factor-induced but not basic fibroblast growth factor-induced angiogenesis. *J. Clin. Invest.*, **99**, 2625-2634, 1997.

[14] Papapetropoulos, A., García-Cardeña, G., Madri, J.A., and Sessa, W.C.: Nitric oxide production contributes to the angiogenic properties of vascular endothelial growth factor in human endothelial cells. *J. Clin. Invest.*, **100**, 3131-3139, 1997.

[15] Park, K.M., Byun, J.Y., Kramers, C., Kim, J.I., Huang, P.L., and Bonventre, J.V.: Inducible nitoric-oxide synthase is an important contributor to prolonged protective effects of ischemic preconditioning in the mouse kidney. *J. Biol. Chem.*, **278**, 27256-27266, 2003.

[16] Murohara, T., Asahara, T., Silver, M., Bauters, C., Masuda, H., Kalka, C., Kearney, M., Chen, D., Symes, J.F., Fishman, M.C., Huang, P.L., and Isner, J.M.: Nitric oxide synthase modulates angiogenesis in response to tissue ischemia. *J. Clin. Invest.*, **101**, 2567-2578, 1998.

[17] Brevetti, L.S., Chang, D.S., Tang, G.L., Sarkar, R., and Messina, L.M.: Overexpression of endothelial nitric oxide synthase increases skeletal muscle blood flow and oxygenation in severe rat hind limb ischemia. *J. Vasc. Surg.*, **38**, 820-826, 2003.

[18] Wildhirt, S.M., Suzuki, H., Horstman, D., Weismüller, S., Dudek, R.R., Akiyama, K., and Reichart, B.: Selective modulation of inducible nitric oxide synthase isozyme in myocardial infarction. *Circulation*, **96**, 1616-1623, 1997.

[19] Misko, T.P., Moore, W.M., Kasten, T.P., Nickols, G.A., Corbett, J.A., Tilton, R.G., McDaniel, M.L., Williamson, J.R., and Currie, M.G.: Selective inhibition of the inducible nitric oxide synthase by aminoguanidine. *Eur. J. Pharmacol.*, **233**, 119-125, 1993.

[20] Joly, G.A., Ayres, M., Chelly, F., and Kilboum, R.G.: Effects of NG-methyl-L-arginine, NG-nitro-L-arginine, and aminoguanidine on constitutive and inducible nitric oxide synthase in rat aorta. *Biochem. Biophys. Res. Commun.*, **199**, 147-154, 1994.

[21] Cross, A.H., Misko T.P., Lin, R.F., Hickey, W.F., Trotter, J.L., and Tilton, R.G.: Aminoguanidine, an inhibitor of inducible nitric oxide synthase, ameliorates experimental autoimmune encephalomyelitis in SJL mice. *J. Clin. Invest.*, **93**, 2684-2690, 1994.

[22] Niu, X.L., Yang, X., Hoshiai, K., Tanaka, K., Swamura, S., Koga, Y., and Nakazawa, H.: Inducible nitric oxide synthase deficiency dose not affect the susceptibility of mice to atherosclerosis but increases collagen content in lesions. *Circulation*, **103**, 1115-1120, 2001.

[23] Wolff, D.J., Gauld, D.S., Neulander, M.J., and Southan, G.: Inactivation of nitric oxide synthase by substituted aminoguanidines and aminoisothioureas. *J. Pharmacol. Exp. Ther.*, **283**, 265-273, 1997.

[24] Wildhirt, S.M., Schulze, C., Conrad, N., Kornberg, A., Horstman, D., and Reichart, B.: Aminoguanidine inhibits inducible NOS and reverses cardiac dysfunction late after ischemia and reperfusion-implications for iNOS-mediated myocardial stunning. *Thorac. Cardiovasc. Surg.*, **47**, 137-143, 1999.

[25] Tamarat, R., Silvestre, J.S., Huijberts, M., Benessiano, J., Ebrahimian, T.G., Duriez, M., Wautier, M.P., Wautier, J.L., and Lévy, B.I.: Blockade of advanced glycation end-product formation restores ischemia-induced angiogenesis in diabetic mice. *Proc. Natl. Acad. Sci. U. S. A.*, **100**, 8555-8560, 2003.

[26] Couffinhal, T., Silver, M., Zheng, L.P., Kearney, M., Witzenbichler, B., and Isner, J.M.: Mouse model of angiogenesis. *Am. J. Pathol.*, **152**, 1667-1679, 1998.

[27] Kasahara, H., Tanaka, E., Fukuyama, N., Sato, E., Sakamoto, H., Tabata, Y., Ando, K., Iseki, H., Shinozaki, Y., Kimura, K., Kuwabara, E., Koide, S., Nakazawa, H., and Mori, H.: Biodegradable gelatin hydrogel potentiates the angiogenic effect of fibroblast growth factor 4 plasmid in rabbit hindlimb ischemia. *J. Am. Coll. Cardiol.*, **41**, 1056-1062, 2003.

[28] Tanaka, E., Hattan, N., Ando, K., Ueno, H., Sugio, Y., Mohammed, M.U., Voltchikhina, S.A., and Mori H.: Amelioration of microvascular myocardial ischemia by gene transfer of vascular endothelial growth factor in rabbits. *J. Thorac. Cardiovasc. Surg.*, **120**, 720-728, 2000.

[29] Lindén, M., Sirsjö, A., Lindbom, L., Nilsson, G., and Gidlöf, A.: Laser-Doppler perfusion imaging of microvascular blood flow in rabbit tenuissimus muscle. *Am. J. Physiol. Heart Circ. Physiol.*, **269**, H1496-H1500, 1995.

[30] Kuwabara, E., Furuyama, F., Ito, K., Tanaka, E., Hattan, N., Fujikura, H., Kimura, K., Goto, T., Hayashi, T., Taira, H., Shinozaki, Y., Umetani, K., Hyodo, K., Tanioka, K., Mochizuki, R., Kawai, T., Koide, S., and Mori, H.: Inhomogeneous vasodilatory responses of rat tail arteries to heat stress: evaluation by synchrotron radiation microangiography. *Jpn. J. Physiol.*, **52**, 403-408, 2002.

[31] Sekka, T., Volchikhina, S.A., Tanaka, A., Hasegawa, M., Tanaka, Y., Ohtani, Y., Tajima, T., Makuuchi, H., Tanaka, E., Iwata, Y., Sato, S., Hyodo, K., Ando, M., Umetani, K., Kubota, M., Tanioka, K., and Mori, H.: Visualization, quantification and therapeutic evaluation of angiogenic vessels in cancer by synchrotron microangiography. *J. Synchrotron Rad.*, **7**, 361-367, 2000.

[32] Takeshita, S., Zheng, L.P., Brogi, E., Kearney, M., Pu, L.G., Bunting, S., Ferrara, N., Symes, J.F., and Isner, J.M.: Therapeutic angiogenesis: a single intra-arterial bolus of vascular endothelial growth factor augments revascularization in a rabbit ischemic hind limb model. *J. Clin. Invest.*, **93**, 662-670, 1994.

[33] Takeshita, S., Isshiki, T., Ochiai, M., Eto, K., Mori, H., Tanaka, E., Umetani, K. and Sato, T.: Endothelium-dependent relaxation of collateral microvessels after intramuscular gene transfer of vascular endothelial growth factor in a rat model of hindlimb ischemia. *Circulation*, **98**, 1261-1263, 1998.

[34] Chung, N.A.Y., Lydakis, C., Belgore, F., Blann, A.D., and Lip, G.Y.H.: Angiogenesis in myocardial infarction An acute or chronic process? *Eur. Heart J.*, **23**, 1604-1608, 2002.

[35] Gavin, J.B., Maxwell, L., and Edgar, S.G.: Microvascular Involvement in Cardiac Pathology. *J. Mol. Cell. Cardiol.*, **30**, 2531-2540, 1998.

[36] Sennlaub, F., Courtois, Y., and Goureau, O. Inducible nitric